Cells with Treg-specific *FOXP3* demethylation but low CD25 are prevalent in autoimmunity

Ricardo C. Ferreira[1,2], Henry Z. Simons[2], Whitney S. Thompson[2], Daniel B. Rainbow[1,2], Xin Yang[2], Antony J. Cutler[1,2], Joao Oliveira[2], Xaquin Castro Dopico[2], Deborah J. Smyth[2], Natalia Savinykh[2], Meghavi Mashar[2], Tim Vyse[3], David B Dunger[4], Helen Baxendale[5], Anita Chandra[5], Chris Wallace[2], John A Todd[1,2], Linda S. Wicker[1,2‡] and Marcin L. Pekalski[1,2‡].

[1]JDRF/Wellcome Trust Diabetes and Inflammation Laboratory, Wellcome Trust Centre for Human Genetics, Nuffield Department of Medicine, NIHR Oxford Biomedical Research Centre, University of Oxford, Oxford, UK. [2]JDRF/Wellcome Trust Diabetes and Inflammation Laboratory, Wellcome Trust/MRC Building, Cambridge Institute for Medical Research, University of Cambridge, Cambridge Biomedical Research Campus, Cambridge, UK. [3]Department of Medical and Molecular Genetics, King's College Hospital, London, UK. [4]Department of Paediatrics, School of Clinical Medicine, University of Cambridge, Cambridge, UK. [5]Department of Clinical Biochemistry and Immunology, Addenbrooke's Hospital, Cambridge, UK.

‡Corresponding Authors:

Prof Linda S Wicker:

Wellcome Trust Centre for Human Genetics, Nuffield Department of Medicine, University of Oxford, Oxford, UK

Email: linda.wicker@well.ox.ac.uk

Dr Marcin L Pekalski:

Wellcome Trust Centre for Human Genetics, Nuffield Department of Medicine, University of Oxford, Oxford, UK

Email: marcin.pekalski@well.ox.ac.uk

29 **Highlights:**

30 - FOXP3^{+} compartment within CD127^{low}CD25^{low} T cells is expanded in autoimmune

31 patients.

32 - Increased numbers of CD25^{low}FOXP3^{+} T cells are a circulating marker of autoimmunity.

33 - CD25^{low}FOXP3^{+} HELIOS^{+} T cells are fully demethylated at the *FOXP3* TSDR.

34 - CD25^{low}FOXP3^{+} T cells could represent a terminal stage of regulatory T cells.

35

36

Abstract

Identification of alterations in the cellular composition of the human immune system is key to understanding the autoimmune process. Recently, a subset of $FOXP3^+$ cells with low CD25 expression was found to be increased in peripheral blood from systemic lupus erythematosus (SLE) patients, although its functional significance remains controversial. Here we find in comparisons with healthy donors that the frequency of $FOXP3^+$ cells within $CD127^{low}CD25^{low}$ $CD4^+$ T cells (here defined as $CD25^{low}FOXP3^+$ T cells) is increased in patients affected by autoimmune disease of varying severity, from combined immunodeficiency with active autoimmunity, SLE to type 1 diabetes. We show that $CD25^{low}FOXP3^+$ T cells share phenotypic features resembling conventional $CD127^{low}CD25^{high}FOXP3^+$ Tregs, including demethylation of the Treg-specific epigenetic control region in *FOXP3* that is highly enriched in $HELIOS^+$ cells, and lack of IL-2 production. As compared to conventional Tregs, more $CD25^{low}FOXP3^+HELIOS^+$ T cells are in cell cycle (33.0% vs 20.7% $Ki\text{-}67^+$; $P = 1.3 \times 10^{-9}$) and express the late-stage inhibitory receptor PD-1 (67.2% vs 35.5%; $P = 4.0 \times 10^{-18}$), while having reduced expression of the early-stage inhibitory receptor CTLA-4, as well as other Treg markers, such as FOXP3 and CD15s. The number of $CD25^{low}FOXP3^+$ T cells are highly correlated ($P = 1.2 \times 10^{-19}$) with the proportion of $CD25^{high}FOXP3^+$ T cells in cell cycle ($Ki\text{-}67^+$). These findings suggest that $CD25^{low}FOXP3^+$ T cells represent a subset of Tregs that are derived from $CD25^{high}FOXP3^+$ T cells, and are a peripheral marker of recent Treg expansion in response to an autoimmune reaction in tissues.

Keywords: Regulatory T cells (Tregs); Autoimmunity; FOXP3; Treg-specific demethylated region (TSDR); CD25.

1. Introduction

FOXP3$^+$ regulatory T cells (Tregs) are produced in the thymus as a specific T cell lineage following high affinity TCR engagement that results in the demethylation of the Treg-specific demethylated region (TSDR) in *FOXP3* and stable FOXP3 expression [1]. Following emigration from the thymus and activation, naïve Tregs proliferate and differentiate to memory Tregs that are actively recruited to peripheral compartments to suppress immune responses against self and maintain tissue integrity [2]. It is becoming increasingly apparent that there is considerable heterogeneity in memory Treg subsets in humans [3,4]. One major challenge for studying human Tregs is that normally only peripheral blood cells from patients are available, rather than the effector T cells and Tregs present in the inflamed tissue and associated lymph nodes. A better understanding of the composition of the Treg compartment in peripheral blood is therefore needed to investigate the potential contribution to disease mechanisms made by Tregs and to identify cellular alterations of the peripheral compartment associated with the onset of pathogenic autoimmune manifestations in the tissues.

Recently, a novel subset of FOXP3$^+$ cells with low expression of CD25 was reported to be increased in peripheral blood of autoimmune systemic lupus erythematosus (SLE) patients [5–9], a finding that was later expanded to the peripheral blood of multiple sclerosis [10] and rheumatoid arthritis [11] patients. The frequency of this cell subset has been demonstrated to be associated with increased disease activity in SLE patients [5–7], suggesting that these cells may be directly pathogenic or biomarkers of flaring autoimmunity. However, the origin of these cells and their function in SLE patients and healthy individuals remain ambiguous [12,13]. In the present study, we characterise these CD127^{low}CD25^{low}FOXP3$^+$ CD4$^+$ T cells

(henceforth designated as $CD25^{low}FOXP3^{+}$ cells), and demonstrate that they share phenotypic features with Tregs, including demethylation of the *FOXP3* TSDR and constitutive expression of the transcription factor HELIOS in a majority of the cells, and an inability to produce IL-2 compared to $FOXP3^{-}$ Teffs. However, compared to conventional $CD127^{low}CD25^{high}FOXP3^{+}$ Tregs, $CD25^{low}FOXP3^{+}$ cells showed increased expression of activation and proliferation markers such as PD-1 and Ki-67, and reduced expression of Treg-associated molecules, including FOXP3 and CTLA-4. We suggest that these cells represent the last stage of the natural life-cycle of TSDR-demethylated Tregs *in vivo* and that active autoimmunity increases their prevalence.

2. **Methods**

2.1 Subjects.

Study participants included 34 SLE patients recruited from Guy's and St Thomas' NHS Foundation Trust. All patients satisfied ACR SLE classification criteria and were allocated a disease activity using SLEDAI-2K at the time of sampling. SLE patients were compared to a cohort of 24 age- and sex-matched healthy donors from the Cambridge BioResource (CBR). A second cohort of 112 healthy donors from the CBR was used for the analysis of Ki-67 expression within the assessed T cell subsets.

Combined immunodeficiency patients (CID; N=7) were recruited from Cambridge University Hospitals and Papworth Hospital NHS Foundation Trusts, and compared to six age- and sex-matched healthy donors from the CBR. Patients were selected on the presentation of immune infiltration in the lungs and active autoimmunity in the absence of a known genetic cause, although the clinical symptoms were consistent with those associated with recently characterised *CTLA4* germline mutations [14].

Adult long-standing T1D patients (N=15) and healthy controls (HC; N=15) were recruited from the CBR. Newly diagnosed T1D patients (ND; N=49) and unaffected siblings of other T1D probands (N=40) were collected from the JDRF Diabetes–Genes, Autoimmunity and Prevention (D-GAP) study (http://paediatrics.medschl.cam.ac.uk/research/clinical-trials/). ND patients were characterised as having been diagnosed with T1D less than two years prior to their blood donation (with one exception of 42 months). Unaffected siblings were islet autoantibody-negative (IAA, IA2, GAD and ZnT8), and were not related to any T1D patient included in this study. All donors were of white ethnicity and all healthy controls and

unaffected siblings were individuals without autoimmune disease (self-reported). Baseline characteristics for all participating subjects are summarised in **Table 1**.

2.2 Ethics.

All samples and information were collected with written and signed informed consent. The D-GAP study was approved by the Royal Free Hospital & Medical School research ethics committee; REC (08/H0720/25). Adult long-standing T1D patients and healthy volunteers were enrolled in the CBR. The study was approved by the local Peterborough and Fenland research ethics committee (05/Q0106/20). Informed consent was obtained from CID patients, parents, or both (R&D Ref: P01685, REC Ref: 12/WA/0148). The study conformed to the Declaration of Helsinki and all local ethical requirements.

2.3 PBMC sample preparation.

PBMCs were isolated by Ficoll gradient centrifugation and cryopreserved in 10% heat-inactivated human AB serum, as described previously [15]. T1D patients and healthy controls were recruited contemporaneously and samples were processed and stored by the same investigators to prevent spurious findings caused by differential sample preparation.

Cryopreserved PBMCs ($10x10^6$ per donor) were thawed at 37°C and resuspended in X-VIVO (Lonza) + 1% heat-inactivated, filtered human AB serum (Sigma). Cell viability following resuscitation was assessed in a subset of 40 donors using the Fixable Viability Dye eFluor 780 (eBioscience) and was found to be consistently very high (95.6%; min = 86.8%, max = 98.2%) for all samples analysed in this study.

2.4 Cell culture and in vitro stimulation.

To reduce the effects of experimental variation and other potential covariates, PBMC samples were processed in batches of a minimum of ten samples per day. T1D patients and healthy controls were matched as closely as possible for age (within 5 year age-bands), sex and time of sample preparation.

After thawing, PBMCs were resuspended in RPMI medium (Gibco) supplemented with 10% FBS, 2 mM L-Glutamine and 100 µg/mL Pen-Strep and cultured (10^6 PBMCs/well) in 24-well flat-bottom cell culture plate (BD). For cytokine production assays, cells were initially rested for 30 min at 37ºC and then cultured in the presence or absence of 5 ng/mL PMA, 100 ng/mL ionomycin and 0.67 µl/mL Monensin GolgiStop (BD Biosciences) for four hours at 37 °C. For a subset of 66 donors, 10^6 cells were cultured with medium alone and 0.67 µl/mL Monensin to determine background levels of cytokine production in unstimulated cells.

2.5 Intracellular immunostainings.

After activation, PBMCs were harvested, and stained with Fixable Viability Dye eFluor 780 for 20 min at 4°C. Cells were then stained with fluorochrome-conjugated antibodies against surface receptors (see **Supplementary Table 1**) for one hour at 4°C. Fixation and permeabilisation was performed using FOXP3 Fix/Perm Buffer Set (BioLegend) and cells were then stained with intracellular antibodies for one hour at 4°C (see **Supplementary Table 1).** All experiments were performed in an anonymised, blinded manner without prior knowledge of disease state.

2.6 Flow cytometry.

166 Immunostained samples were acquired using a BD Fortessa (BD Biosciences) flow cytometer
167 with FACSDiva software (BD Biosciences) and analysed using FlowJo (Tree Star, Inc.).
168 Dead-cell exclusion based on the Fixable Viability Dye was performed for the intracellular
169 immunostainings.
170
171 *2.7 Analysis of the epigenetic demethylation profile by next-generation sequencing.*
172 Total PBMCs from seven healthy CBR donors (three males and four females) were stained
173 with fluorophore-conjugated antibodies (see **Supplementary Table 1**) and sorted using a BD
174 Aria Fusion flow cytometer (BD Biosciences). Methylation of the *FOXP3* TSDR was
175 performed using a next-generation sequencing method, as described previously [16].
176
177 *2.8 Statistical analyses.*
178 Statistical analyses were performed using Prism software (GraphPad) and Stata
179 (www.stata.com). Association of the assessed T-cell phenotypes with T1D, SLE and CID
180 was calculated using two-tailed unpaired student's t-tests. The effects of age, sex and time of
181 collection were controlled by the experimental design used in this study and, therefore, not
182 included as additional covariates. Given that most immune phenotypes showed moderate to
183 strong right skew that violated the assumption of normality, the phenotypes were log-
184 transformed before statistical testing.
185
186 Comparison of the expression of the interrogated immune markers between
187 $CD127^{low}CD25^{low}FOXP3^{+}$ $CD4^{+}$ T cells and: (i) $CD25^{high}FOXP3^{+}$, (ii) $CD25^{high}FOXP3^{-}$ and
188 (iii) $CD25^{low}FOXP3^{-}$ $CD4^{+}$ T cells was performed within individuals using two-tailed paired
189 student's t-tests. The correlations between immune subsets were calculated using linear

190 regression analysis.

191

3. Results

3.1 Frequency of CD25^{low}FOXP3^{+} cells is increased in blood from patients with active autoimmunity.

To investigate the peripheral alterations in peripheral FOXP3^{+} T cell subsets, we performed a detailed immunophenotyping characterisation of cryopreserved peripheral blood mononuclear cells (PBMCs) of different cohorts of autoimmune patients (summarised in **Table 1**). Analysis of the flow cytometry profile of patients with systemic autoimmune manifestations as compared to healthy donors revealed that the frequency of FOXP3^{+} cells is highly increased in CD127^{low} cells of some patients. We found that among SLE and CID patients with increased CD127^{low} FOXP3-expressing cells there is a notable loss of CD25 expression, which results in an extremely high frequency of CD127^{low}CD25^{low}FOXP3^{+} cells (**Fig. 1A**). These findings suggest that the frequency of FOXP3^{+} cells in the CD127^{low}CD25^{low} T cell subset (CD25^{low}FOXP3^{+} cells; depicted in red in **Fig. 1B**) is increased as a result of an active autoimmune response and could be a specific marker of Treg activation. Given the lack of peripheral markers that reflect chronic immune activation, we therefore decided to focus our analysis on this population of CD25^{low}FOXP3^{+} cells, and investigate their frequency in the peripheral blood of autoimmune patients.

Consistent with previous findings [7,8], we confirmed that the frequency of FOXP3^{+} cells among CD127^{low}CD25^{low} T cells (gating strategy **Fig. 1B**) was markedly increased in SLE patients (geometric mean (GeoM) = 13.53%) compared to age- and sex-matched healthy controls (5.51%, $P = 2.1 \times 10^{-5}$, N = 24, **Fig. 1C**), which likely reflects the systemic immune activation in SLE patients. In support of this hypothesis, we also detected a high frequency

of $CD25^{low}FOXP3^{+}$ cells in a small cohort of seven CID patients, characterised by severe active autoimmunity compared to age- and sex-matched healthy controls (12.14% and 4.00%, respectively, $P = 6.5 \times 10^{-3}$; **Fig. 1C**).

We also found that the frequency of $FOXP3^{+}$ cells among $CD127^{low}CD25^{low}$ T cells was significantly increased in T1D patients (6.84%) compared to age- and sex-matched healthy controls (4.55%; $P = 2.7 \times 10^{-6}$; **Fig. 1D**). This association was also observed when comparing the frequency of $CD25^{low}FOXP3^{+}$ cells within total $CD4^{+}$ T cells (0.32% vs 0.23% in T1D patients and controls, respectively; $P = 1.1 \times 10^{-3}$; **Supplementary Fig. 1A**), and was not associated with duration of disease, ranging from 2 months to 23 years (P = 0.61). We replicated the finding of increased $FOXP3^{+}$ cells among $CD127^{low}CD25^{low}$ T cells in an independent cohort of 15 long-standing T1D patients (10.39%) and 15 age- and sex-matched healthy controls (6.29%; $P = 7.7 \times 10^{-3}$; **Supplementary Fig. 1B**). Furthermore, we noted that the increased frequency of $FOXP3^{+}$ cells was mainly restricted to the $CD127^{low}CD25^{low}$ T cell subset, as we observed only a small increased frequency of conventional $CD127^{low}CD25^{high}FOXP3^{+}$ Tregs in T1D patients (5.55%) compared to healthy donors (4.82%; $P = 8.0 \times 10^{-3}$; **Supplementary Fig. 2**).

3.2 $CD25^{low}FOXP3^{+}$ cells are demethylated at the FOXP3 TSDR.

In humans FOXP3 is not exclusively expressed in Tregs, but can also be transiently up-regulated in activated Teffs. However, in thymically-derived Tregs constitutive expression of *FOXP3* is known to require a demethylated TSDR [2]. To assess the TSDR methylation profile of $CD25^{low}FOXP3^{+}$ cells we sorted these cells from four healthy donors, and compared the methylation of the TSDR in $CD25^{low}FOXP3^{+}$ cells, conventional

CD25^{high}FOXP3^{+} Tregs and the respective FOXP3^{-} subsets (**Fig. 2A**). We found that the majority of CD25^{low}FOXP3^{+} cells were demethylated at the TSDR (**Fig. 2B,C**). The epigenetic demethylation pattern in CD25^{low}FOXP3^{+} cells was similar to CD25^{high}FOXP3^{+} Tregs at all nine interrogated CpG sites in the *FOXP3* TSDR (mean = 57.1% and 80.5% demethylation, respectively; **Fig. 2B**); in contrast, <7% of CD25^{low}FOXP3^{-} and CD25^{high}FOXP3^{-} cells had demethylated TSDRs. These findings indicate the majority of CD25^{low}FOXP3^{+} cells are *bona fide* Tregs, and are not Teffs transiently upregulating FOXP3 expression as a result of immune activation.

3.3 CD25^{low}FOXP3^{+} cells express the Treg-specific HELIOS transcription factor and exhibit features of an activated phenotype.

Having established that a majority of CD25^{low}FOXP3^{+} cells are stably demethylated at the *FOXP3* TSDR, we next performed a detailed phenotypic characterisation of this immune subset by flow cytometry in 24 healthy adult donors to investigate phenotypic similarities and differences between CD25^{low}FOXP3^{+} and classical Tregs (CD25^{high}FOXP3^{+}). One distinguishing feature of these cells was the higher frequency of memory phenotype (CD45RA^{-}) cells compared to their CD25^{high}FOXP3^{+} counterparts (83.8% and 64.7% CD45RA^{-} cells, respectively; $P = 2.0 \times 10^{-11}$; **Fig. 3A**). This difference was particularly noticeable among the younger cohort (median age = 14 years) of 116 T1D patients and unaffected siblings (76.9% and 43.4%, respectively; $P = 1.2 \times 10^{-58}$; **Fig. 3B**), which have a higher proportion of CD45RA^{+} naïve cells amongst their CD25^{high}FOXP3^{+} conventional Tregs compared to adult donors, suggesting that the majority of CD25^{low}FOXP3^{+} cells have responded previously to antigen following their emigration from the thymus. Since the majority of CD25^{low}FOXP3^{+} cells are CD45RA^{-}, we focused further analyses on memory

264 FOXP3$^+$ cells.

265

266 We found that an increased frequency of CD45RA$^-$ CD25^{low}FOXP3$^+$ cells express the
267 proliferation marker Ki-67 compared to their CD25^{high}FOXP3$^+$ counterparts (29.9% and
268 22.0%, respectively; $P = 2.7 \times 10^{-7}$; **Fig. 3C**). In addition to Ki-67, CD45RA$^-$
269 CD25^{low}FOXP3$^+$ cells were also characterised by a marked increased frequency of PD-1$^+$
270 cells compared to CD25^{high}FOXP3$^+$ Tregs (65.1% and 38.3%, respectively; $P = 1.7 \times 10^{-17}$;
271 **Fig. 3D**), and had a frequency of PD-1$^+$ cells more similar to their CD25^{low}FOXP3$^-$
272 counterparts (67.2%; **Fig. 3D**).

273

274 Furthermore, we demonstrated that, similarly to CD25^{high}FOXP3$^+$ CD45RA$^-$ memory Tregs,
275 the majority of CD25^{low}FOXP3$^+$ CD45RA$^-$ memory cells also express the transcription factor
276 HELIOS, although the proportion of HELIOS$^+$ cells was significantly lower (51.1%)
277 compared to CD25^{high}FOXP3$^+$ CD45RA$^-$ memory Tregs (77.8%; $P = 3.0 \times 10^{-12}$; **Fig. 4A,**
278 **B)**. Consistent with the reduction in CD25 and HELIOS, CD25^{low}FOXP3$^+$ cells also showed
279 a significantly lower expression of other classical Treg markers compared to
280 CD25^{high}FOXP3$^+$ Tregs, such as TIGIT (65.1% vs 78.0%; $P = 3.7 \times 10^{-8}$), CD15s **(**20.7% vs
281 33.5%; $P = 5.8 \times 10^{-12}$) and most notably, CTLA-4 (60.0% vs 84.7%; $P = 9.4 \times 10^{-11}$; **Fig.**
282 **4A, B)**. Furthermore, we found that the expression of FOXP3 was markedly lower in
283 CD25^{low}FOXP3$^+$ cells compared to CD25^{high}FOXP3$^+$ Tregs (MFI = 1171 and 2160
284 respectively, $P = 3.6 \times 10^{-11}$; **Fig. 4C**), suggesting that CD25^{low}FOXP3$^+$ cells show a
285 decreased expression of classical Treg-associated molecules.

286

287 *3.4 HELIOS$^+$CD45RA$^-$ CD25^{low}FOXP3$^+$ cells are demethylated at the FOXP3 TSDR to the*

same degree as conventional HELIOS$^+$CD45RA$^-$ CD25^{high} FOXP3$^+$ Tregs.

To further investigate the methylation profile of FOXP3$^+$ cells, we next assessed the TSDR methylation in the HELIOS$^+$ and HELIOS$^-$ subsets in three additional healthy donors. In agreement with their putative Treg lineage, we confirmed that the HELIOS$^+$ subsets of both CD25^{low}FOXP3$^+$ cells and conventional CD25^{high}FOXP3$^+$ Tregs are virtually completely demethylated at the *FOXP3* TSDR (>95%; **Fig. 5A**). In contrast, the HELIOS$^-$ subsets of CD25^{low}FOXP3$^+$ cells and conventional CD25^{high}FOXP3$^+$ Tregs showed a much lower portion of cells demethylated at the TSDR (21% and 64%, respectively). Since HELIOS expression is highly enriched in FOXP3$^+$ cells demethylated at the TSDR, we examined other phenotypes within the FOXP3$^+$ cells stratified by HELIOS expression. CD25^{low}FOXP3$^+$ cells demethylated at the TSDR as defined by HELIOS expression had a higher proportion in cell cycle as compared to CD25^{high}FOXP3$^+$ cells expressing HELIOS (33.0% and 20.7%, respectively; **Fig. 5B,C**). In addition, the proportion of cells expressing PD-1 and the per cell level of PD-1 were both increased on CD25^{low}FOXP3$^+$ demethylated at the TSDR as compared to their CD25^{high} counterparts (**Fig. 5B,C**). Expression of TIGIT, CTLA-4 and CD15s were also compared **(Supplementary Fig. 3)** with HELIOS stratification revealing a high percentage (>89%) of TIGIT$^+$ cells in both populations of demethylated FOXP3$^+$ cells, but a reduced number expressing CD15s and CTLA-4 in the CD25^{low}FOXP3$^+$ cells demethylated at the TSDR as compared to their CD25^{high} counterparts. High expression of CTLA-4 was present on CD25^{high}FOXP3$^+$HELIOS$^-$ cells, a population with >50% of the cells having a demethylated TSDR (**Fig. 5A**). Expression of FOXP3 was found to be significantly higher within both conventional CD25^{high} Tregs (MFI > 2100) compared to CD25^{low}FOXP3$^+$ HELIOS$^+$ T cells (MFI = 1590), despite their demethylated TSDR. Notably, the expression of FOXP3 was markedly lower in CD25^{low}FOXP3$^+$ HELIOS$^-$ T cells

(MFI = 952), which is consistent with their methylated TSDR **(Supplementary Fig. 3)**. Furthermore, analysis of $CD45RA^+$ expression revealed a significantly lower frequency of $CD45RA^+$ cells within total $CD25^{low}FOXP3^+$ $HELIOS^+$ cells (4.7%) compared to their $CD25^{high}$ counterparts (20.8%; $P = 2.0 \times 10^{-12}$; **Supplementary Fig. 3**). These data suggest that most of the $CD45RA^+$ cells observed within $CD25^{low}FOXP3^+$ T cells are memory effector T cells that have re-expressed CD45RA on their surface and are characterized by being $HELIOS^-$ and expressing lower levels of FOXP3. Finally, since it was possible that the expansion of $CD25^{low}FOXP3^+$ $HELIOS^-$ cells (most of which lack a demethylated TSDR and might be activated effector cells) could have been responsible for the increase of $CD25^{low}FOXP3^+$ cells in autoimmune patients **(Fig. 1B,C)**, we examined the distribution of $HELIOS^+$ and $HELIOS^-$ cells within the $CD25^{low}FOXP3^+$ subset. We determined that $HELIOS^+$ $CD25^{low}FOXP3^+$ cells were increased in SLE, CID and T1D patients as compared to their healthy control cohorts **(Supplementary Fig. 4A,B)** similar to the findings with $CD25^{low}FOXP3^+$ cells **(Fig. 1C,D)** and that $HELIOS^+$ cells contributed significantly to all cohorts examined **(Supplementary Fig. 4C,D).**

3.5 Low IL-2 production from $HELIOS^+CD45RA^-$ $CD25^{low}FOXP3^+$ cells.

To characterise the function of $HELIOS^+CD45RA^-$ $CD25^{low}FOXP3^+$ cells, we assessed the production of two key cytokines, IL-2 and IFN-γ, in ten donors (five T1D patients and five healthy controls) following *in vitro* stimulation (**Fig. 6**). Consistent with their Treg-like phenotype, we found that both the $HELIOS^+CD45RA^-$ $CD25^{low}FOXP3^+$ and $CD25^{high}FOXP3^+$ subsets, which are highly demethylated at the TSDR (**Fig. 5A**), showed a low frequency of $IL\text{-}2^+$ (2.0% and 1.0%, respectively) and $IFN\text{-}\gamma^+$ cells (5.1% and 1.4%, respectively; **Fig. 6B,C**). This was in marked contrast with the $HELIOS^+CD25^{low}FOXP3^-$

subset, which was found to secrete significantly higher levels of both IL-2 (21.3%; $P = 2.8 \times 10^{-5}$; **Fig. 6B**) and IFN-γ (27.9%; $P = 1.1 \times 10^{-3}$; **Fig. 6C**), compared their $FOXP3^+$ counterparts (2.0% and 5.1% for IL-2 and IFN-γ, respectively). In agreement with their regulatory phenotype, we found a strong reduction of $IL\text{-}2^+$ and $IFN\text{-}\gamma^+$ cells (2.0% and 5.1%, respectively) in $HELIOS^+CD45RA^-$ $CD127^{low}CD25^{low}FOXP3^+$ cells compared to conventional Teffs (59.8%, $P = 5.3 \times 10^{-9}$ and 63.5%, $P = 2.0 \times 10^{-7}$ for $IL\text{-}2^+$ and $IFN\text{-}\gamma^+$ cells, respectively; **Fig. 6B,C**).

As compared to the $HELIOS^+$ fraction, we found that a higher portion of $HELIOS^-$ $CD45RA^-$ $CD25^{low}FOXP3^+$ cells produced IFN-γ **(Fig. 6A, Supplementary Fig. 5A)**. These findings are consistent with a previous study, showing that $HELIOS^-FOXP3^+$ T cells produced IFN-γ, and were increased among T1D patients [17]. Although we found no evidence for differential IFN-γ production in T1D patients compared to healthy controls among $HELIOS^-$ $CD45RA^-CD127^{low}CD25^{low}FOXP3^+$ cells, on a per cell basis (**Supplementary Fig. 5B**), the higher frequency of the $CD25^{low}FOXP3^+$ subset among patients resulted in a significant increase in the frequency of circulating $FOXP3^+$ cells with the capability to produce IFN-γ following stimulation among total $CD4^+$ T cells ($P = 2.5 \times 10^{-3}$; **Supplementary Fig. 5C**). These data suggest that $HELIOS^-$ $CD45RA^-$ $CD127^{low}CD25^{low}FOXP3^+$ cells contributed to the increased frequency of $IFN\text{-}\gamma^+$ cells reported among $FOXP3^+$ cells from T1D patients [17].

3.6 $CD25^{low}FOXP3^+$ T cells are highly correlated with proliferating $CD25^{high}FOXP3^+$ Tregs.

To investigate the possible relationship between $CD25^{high}$ and $CD25^{low}$ $FOXP3^+HELIOS^+$

Tregs, we hypothesized that if $CD25^{high}$ $FOXP3^{+}HELIOS^{+}$ Tregs are the precursors of the $CD25^{low}$ $FOXP3^{+}HELIOS^{+}$ T cell subset, the numbers of $CD25^{high}$ Tregs in cycle ($Ki\text{-}67^{+}$) and $CD25^{low}$ $FOXP3^{+}HELIOS^{+}$ T cells should be correlated. This correlation would be required to maintain homeostasis of Treg numbers such that as memory $CD25^{high}$ Tregs are required to increase in peripheral compartments to respond to inflammatory conditions, a higher Treg turnover would lead to more $CD25^{high}$ Tregs moving into the $CD25^{low}$ compartment and ultimately to cell death. We assessed the total numbers of $CD45RA^{-}$ $Ki\text{-}67^{+}$ Tregs both in the cohort of 24 healthy volunteers (cohort 1) and in an independent replication cohort (cohort 2) of 112 healthy volunteers. We found that the frequency of $CD45RA^{-}$ $CD4^{+}$ $Ki\text{-}67^{+}$ $CD25^{high}FOXP3^{+}HELIOS^{+}$ Tregs was significantly correlated with the frequency of $CD25^{low}FOXP3^{+}HELIOS^{+}$ T cells within total memory $CD4^{+}$ T cells (r^2 = 0.18, $P = 3.1 \times 10^{-7}$; **Fig. 7A**). Similarly, we observed a strong correlation between the numbers of in-cycle $Ki\text{-}67^{+}$ Tregs and the $CD25^{high}FOXP3^{+}HELIOS^{+}$ Treg compartment (r^2 = 0.46, $P = 1.2 \times 10^{-19}$; **Fig. 7B**), as well as a significant correlation between both the total $CD25^{low}$ and $CD25^{high}$ $FOXP3^{+}HELIOS^{+}$ T cell compartments ($r^2 = 0.15$, $P = 3.9 \times 10^{-6}$; **Fig. 7C**). These observed correlations were very consistent within both cohorts of healthy volunteers, and suggest that proliferation of conventional $CD25^{high}$ $FOXP3^{+}HELIOS^{+}$ T cells is critical to promote the homeostatic repopulation of the $CD25^{high}$ Treg subset, which is maintained at a steady state frequency through the progression of a proportion of $CD25^{high}$ Tregs to the $CD25^{low}$ $FOXP3^{+}HELIOS^{+}$ compartment.

4. Discussion

The identification of reliable biomarkers of disease activity has been a major challenge of autoimmune diseases, particularly in organ-specific diseases, such as T1D, where there is limited access to the inflamed tissues. In this study we characterised a subset of $FOXP3^+$ $CD127^{low}CD25^{low}$ T cells, and show that it could be a peripheral biomarker of a recent autoimmune reaction in the tissues. We showed that in addition to SLE, where the increase of $FOXP3^+$ $CD25^{low}$ T cells has been observed in multiple SLE studies [5–9], the proportion of $FOXP3^+$ cells in the $CD127^{low}CD25^{low}$ subset is increased in CID and T1D patients. Although the frequency of $FOXP3^+$ cells in the $CD127^{low}CD25^{low}$ subset was compared in T1D patients versus controls in one previous study with no difference observed [13], we note that the number of participants was small: 10 healthy control individuals and 16 patients. In contrast, Zoka et al [18] observed that the proportion of $CD25^{low}$ cells among $FOXP3^+CD4^+$ T cells is higher in T1D patients than in controls, a phenotype consistent with our observations.

A major strength of this study is that we were able to use a recently developed assay [16] to precisely assess the methylation status of the *FOXP3* TSDR of $CD25^{low}FOXP3^+$ cells, a feature that was lacking in the previous SLE studies [7,8] or studies of this subset from healthy individuals [13]. This method provides a more quantitative assessment of the methylation pattern of the *FOXP3* locus [16] in the different immune subsets, which allowed us to demonstrate that the epigenetic profile of $CD25^{low}FOXP3^+$ cells was remarkably similar to conventional $CD25^{high}$ $FOXP3^+$ Tregs (57.1% and 80.5% demethylated at the TSDR, respectively). We went on to define that this epigenetic similarity was caused primarily by the TSDR methylation status of $HELIOS^+$ cells: virtually all $HELIOS^+$ cells were found to be

404 demethylated in both the $CD25^{high}$ and $CD25^{low}$ $FOXP3^{+}$ subsets. This finding is consistent
405 with a previous study assessing the *FOXP3* TSDR methylation profile in different
406 $CD4^{+}CD127^{low}$ T-cell subsets discriminated by their expression of FOXP3 and CD25 [19].
407 The majority of $CD25^{low}FOXP3^{+}$ cells sorted from synovial fluid mononuclear cells of
408 juvenile idiopathic arthritis patients were shown to have a demethylated *FOXP3* TSDR,
409 suggesting that this subset may be enriched at inflammatory sites [19]. In the current study
410 we also found that the proportion of cells expressing TIGIT was elevated over 2-fold in both
411 $FOXP3^{+}HELIOS^{+}$ subsets as compared to their $FOXP3^{+}HELIOS^{-}$ counterparts. Stable
412 demethylation of the *FOXP3* TSDR occurs in the thymus upon strong T-cell receptor
413 stimulation [1], therefore suggesting that $CD25^{low}$ $FOXP3^{+}HELIOS^{+}$ cells are *bona-fide*
414 thymically-derived Tregs that have lost the expression of CD25.
415
416 In further support of the hypothesis that $CD25^{low}FOXP3^{+}$ $HELIOS^{+}$ T cells are in fact a
417 subset of the classical $FOXP3^{+}$ Treg subset, these cells were unable to produce IL-2
418 following *in vitro* activation. This finding was in contrast with the report by Yang *et al* [8]
419 that $CD25^{low}FOXP3^{+}$ T cells from new-onset SLE patients were able to secrete IL-2.
420 However, we note that the IL-2 production reported in Yang *et al* was much lower compared
421 to $CD25^{high}FOXP3^{-}$ Teffs, and immune subsets were not stratified based on the expression of
422 CD127, CD45RA and HELIOS. It is therefore likely that the residual production of IL-2
423 observed by Yang *et al* in $CD25^{low}FOXP3^{+}$ T cells was due primarily to $HELIOS^{-}$ T cells. In
424 contrast, in our study we demonstrate that $CD45RA^{-}$ $CD25^{low}CD127^{low}$ $HELIOS^{+}FOXP3^{+}$
425 cells have a profound inability to produce IL-2 as compared to $CD127^{+}CD25^{high}$ $CD45RA^{-}$
426 $HELIOS^{-}FOXP3^{-}$ Teffs. We also noted the overall heterogeneity in the $CD127^{low}$ subset in
427 regard to IL-2 and IFN-γ secretion (**Fig. 6**). A similar proportion of $CD127^{low}$ cells lacking

both FOXP3 and HELIOS expression secrete IL-2 and IFN-γ as compared to their $CD127^{+}$ counterparts and are likely effector T cells. In healthy individuals we observed that these putative effector cells are the largest portion of the $CD45RA^{-}$ $CD25^{low}CD127^{low}$ gate (**Fig. 1B**), consistent with previous observations [13].

In addition to reduced levels of CD25, $CD25^{low}$ $HELIOS^{+}FOXP3^{+}$ Tregs had lower expression of CTLA-4, CD15s and FOXP3 as compared to $CD25^{high}$ $HELIOS^{+}FOXP3^{+}$ Tregs, suggesting that $CD25^{low}$ Tregs could have decreased suppressive function. One limitation of our study is that we are not able to directly assess the suppressive capacity of $CD25^{low}$ $HELIOS^{+}FOXP3^{+}$ cells, as sorting on the intracellular transcription factors precludes the use of these cells for functional assays and surrogate surface markers are not yet defined. Also, as described above, the $CD45RA^{-}$ $CD25^{low}CD127^{low}$ gate has a high proportion of effector cells present making the results of suppression experiments using populations of cells gated as $CD25^{low}CD127^{low}$ difficult to interpret. Notably, despite the cellular heterogeneity inherent in the $CD25^{low}CD127^{low}$ subset, two studies did test the suppressive capacity of sorted $CD25^{low}CD127^{low}$ $CD4^{+}$ T cells [7,13]. Suppression of proliferation by Teffs was mediated by $CD25^{low}CD127^{low}$ $CD4^{+}$ T cells in both studies; however IFN-γ secretion by Teffs was not suppressed in the one study that examined this parameter [7]. The reduced suppression mediated by $CD25^{low}CD127^{low}$ $CD4^{+}$ T cells could be due to the fact that a larger proportion of effector cells are present in this subset as compared with their $CD25^{+}$ counterparts. Overall the observation of suppression by $CD25^{low}CD127^{low}$ $CD4^{+}$ T cells supports the conclusion that the $CD25^{low}$ $HELIOS^{+}FOXP3^{+}$ Tregs present in the heterogeneous $CD25^{low}CD127^{low}$ $CD4^{+}$ T cell population are

451 functionally suppressive. Future studies are needed to unravel the heterogeneity present in
452 both the $CD25^{low}$ and $CD25^{high}$ $CD127^{low}CD4^{+}$ T cell subsets.
453
454 In contrast to the reduced expression of several molecules that are abundant in $FOXP3^{+}$
455 Tregs, the frequency of cells expressing PD-1 and Ki-67 in $CD25^{low}$ Tregs was higher than in
456 conventional $CD25^{high}$ Tregs, suggesting that the $CD25^{low}$ $HELIOS^{+}FOXP3^{+}$ population may
457 represent the consequences of $CD25^{high}$ Tregs attempting to suppress ongoing inflammatory
458 responses in tissues. The progression of $CD25^{high}$ Tregs to the $CD25^{low}$ Treg subset is
459 supported by our observation of the strong correlation between the frequency of $CD25^{high}$
460 Tregs in cell cycle ($Ki\text{-}67^{+}$) with the number of $CD25^{low}$ Tregs. The high proportion (15-
461 40%) of memory $FOXP3^{+}$ Tregs in cycle is consistent with their shorter half-lives as
462 compared to other T cell subsets [20,21]. Thus, given the fact that Treg percentages normally
463 remain constant in an individual through time [21], and a high proportion of the cells are
464 replicating, Treg cell death must be a common outcome following cell division. We propose
465 that the decreased expression of CD25 on Tregs, most likely caused by exposure to
466 inflammatory conditions, causes less responsiveness to IL-2, reduced expression of FOXP3
467 and other Treg-associated molecules, and an increased probability of cell death. Despite the
468 reduced IL-2 responsiveness in $CD25^{low}$ Tregs, it is possible that the Tregs remain functional
469 and that the upregulation of PD-1 could compensate for reductions in FOXP3 and CTLA-4
470 levels [22]. Consistent with this hypothesis, previous studies have reported that PD-1 is a
471 critical inhibitory molecule that is upregulated on T cells after activation [23–25]. In contrast,
472 chronic PD-1 signaling within peripheral compartments has been reported to lead to reduced
473 STAT5 phosphorylation, decreased expression of CD25, FOXP3 and CTLA-4, and decreased

474 Treg suppressive function [26–28]. Additional functional studies are required to resolve these

475 apparently contradictory mechanisms.

476

5. Conclusions

We hypothesize that the presence of a low frequency of $CD25^{low}$ $HELIOS^{+}FOXP3^{+}$ cells in peripheral blood from healthy individuals reflects a normal physiological mechanism to maintain, genetically-regulated, Treg levels. Their increased frequency in peripheral blood from autoimmune patients, which is particularly noteworthy in patients with chronic systemic inflammation, is indicative of an inflammatory insult that drives the expansion of the Treg population, which can be transient or chronic, in an attempt to regulate an overt autoimmune Teff response. Given the paucity of reliable peripheral biomarkers of disease activity, our findings suggest that the frequency of $CD25^{low}$ $HELIOS^{+}FOXP3^{+}$ Tregs could provide valuable information about recent or ongoing tissue inflammation and could have a clinical application for the stratification of patients with flaring autoimmunity.

Author contributions

R.C.F., J.A.T., L.S.W. and M.L.P. designed experiments and interpreted data. R.C.F., H.Z.S., W.S.T., D.B.R., A.J.C., J.O., X.C.D., D.J.S., N.S., M.M. and M.L.P. performed experiments. X.Y. analysed the data. C.W. supervised the statistical analysis of the data. T.V., D.B.D., H.B and A.C. provided samples and clinical outcome data. R.C.F., J.A.T., L.S.W. and M.L.P. conceived the study and wrote the paper.

Acknowledgements

This work was supported by the JDRF UK Centre for Diabetes - Genes, Autoimmunity and Prevention (D-GAP; 4-2007-1003) in collaboration with M. Peakman and T. Tree at Kings College London, the JDRF, the Wellcome Trust (WT; WT061858/091157) and the National Institute for Health Research Cambridge Biomedical Research Centre. RCF is funded by an advanced JDRF post-doctoral fellowship (3-APF-2015-88-A-N). CW is funded by the Wellcome Trust (088998).

We thank staff of the National Institute for Health Research (NIHR) Cambridge BioResource recruitment team for assistance with volunteer recruitment and K. Beer, T. Cook, S. Hall and J. Rice of the Cambridge BioResource for blood sample collection. We thank C. Guy from the Department of Paediatrics, School of Clinical Medicine, University of Cambridge for D-GAP sample recruitment. We thank M. Woodburn and T. Attwood from the Cambridge Institute for Medical Research, University of Cambridge for their contribution to sample management and N. Walker and H. Schuilenburg from the Cambridge Institute for Medical Research, University of Cambridge for data management. This research was supported by the Cambridge NIHR BRC Cell Phenotyping Hub. In particular, we wish to thank Anna Petrunkina Harrison, Simon McCullum, Christopher Bowman and Esther Perez from the Cambridge NIHR BRC Cell Phenotyping Hub for their advice and support in cell sorting. We thank Howard Martin, Fay Rodger and Ruth Littleboy for running the Illumina MiSeq in the Molecular Genetics Laboratories, Addenbrooke's Hospital, Cambridge. We thank members of the NIHR Cambridge BioResource SAB and management committee for their support and the NIHR Cambridge Biomedical Research Centre for funding. Access to NIHR Cambridge BioResource volunteers and their data and samples is governed by the NIHR Cambridge BioResource SAB. Documents describing access arrangements and contact details are available at http://www.cambridgebioresource.org.uk/. We also thank H. Stevens, P. Clarke, G. Coleman, S. Dawson, S. Duley, M. Maisuria-Armer and T. Mistry from the Cambridge Institute for Medical Research, University of Cambridge for preparation of PBMC samples.

References

[1] N. Ohkura, M. Hamaguchi, H. Morikawa, K. Sugimura, A. Tanaka, Y. Ito, M. Osaki, Y. Tanaka, R. Yamashita, N. Nakano, J. Huehn, H.J. Fehling, T. Sparwasser, K. Nakai, S. Sakaguchi, T Cell Receptor Stimulation-Induced Epigenetic Changes and Foxp3 Expression Are Independent and Complementary Events Required for Treg Cell Development, Immunity. 37 (2012) 785–799.

[2] M. Miyara, Y. Yoshioka, A. Kitoh, T. Shima, K. Wing, A. Niwa, C. Parizot, C. Taflin, T. Heike, D. Valeyre, A. Mathian, T. Nakahata, T. Yamaguchi, T. Nomura, M. Ono, Z. Amoura, G. Gorochov, S. Sakaguchi, Functional Delineation and Differentiation Dynamics of Human CD4+ T Cells Expressing the FoxP3 Transcription Factor, Immunity. 30 (2009) 899–911.

[3] K. Bin Dhuban, E. D'Hennezel, E. Nashi, A. Bar-Or, S. Rieder, E.M. Shevach, S. Nagata, C.A. Piccirillo, Coexpression of TIGIT and FCRL3 Identifies Helios+ Human Memory Regulatory T Cells, J. Immunol. 194 (2015) 3687–3696.

[4] C.A. Fuhrman, W.-I. Yeh, H.R. Seay, P. Saikumar Lakshmi, G. Chopra, L. Zhang, D.J. Perry, S.A. McClymont, M. Yadav, M.-C. Lopez, H. V Baker, Y. Zhang, Y. Li, M. Whitley, D. von Schack, M.A. Atkinson, J.A. Bluestone, T.M. Brusko, Divergent Phenotypes of Human Regulatory T Cells Expressing the Receptors TIGIT and CD226, J. Immunol. 195 (2015) 145–155.

[5] B. Zhang, X. Zhang, F.L. Tang, L.P. Zhu, Y. Liu, P.E. Lipsky, Clinical significance of increased CD4+CD25−Foxp3+ T cells in patients with new-onset systemic lupus erythematosus, Ann. Rheum. Dis. 67 (2008) 1037–1040.

[6] R.K. Chowdary Venigalla, T. Tretter, S. Krienke, R. Max, V. Eckstein, N. Blank, C. Fiehn, A. Dick Ho, H.-M. Lorenz, Reduced CD4+,CD25− T cell sensitivity to the suppressive function of CD4+,CD25high,CD127−/low regulatory T cells in patients with active systemic lupus erythematosus, Arthritis Rheum. 58 (2008) 2120–2130.

[7] M. Bonelli, A. Savitskaya, C.-W. Steiner, E. Rath, J.S. Smolen, C. Scheinecker, Phenotypic and Functional Analysis of CD4+CD25−Foxp3+ T Cells in Patients with Systemic Lupus Erythematosus, J. Immunol. 182 (2009) 1689–1695.

[8] H. Yang, W. Zhang, L. Zhao, Y. Li, F. Zhang, F. Tang, W. He, X. Zhang, Are CD4+CD25-Foxp3+cells in untreated new-onset lupus patients regulatory T cells?,

Arthritis Res. Ther. 11 (2009) 1–9.

[9] J.-L. Suen, H.-T. Li, Y.-J. Jong, B.-L. Chiang, J.-H. Yen, Altered homeostasis of CD4+ FoxP3+ regulatory T-cell subpopulations in systemic lupus erythematosus, Immunology. 127 (2009) 196–205.

[10] M. Fransson, J. Burman, C. Lindqvist, C. Atterby, J. Fagius, A. Loskog, T regulatory cells lacking CD25 are increased in MS during relapse, Autoimmunity. 43 (2010) 590–597.

[11] B. de Paz, C. Prado, M. Alperi-López, F.J. Ballina-García, J. Rodriguez-Carrio, P. López, A. Suárez, Effects of glucocorticoid treatment on CD25−FOXP3+ population and cytokine-producing cells in rheumatoid arthritis, Rheumatology. 51 (2012) 1198–1207.

[12] D.A. Horwitz, Identity of mysterious CD4+CD25-Foxp3+ cells in SLE, Arthritis Res. Ther. 12 (2010) 101.

[13] W. Liu, A.L. Putnam, Z. Xu-yu, G.L. Szot, M.R. Lee, S. Zhu, P.A. Gottlieb, P. Kapranov, T.R. Gingeras, B.F. de St. Groth, C. Clayberger, D.M. Soper, S.F. Ziegler, J.A. Bluestone, CD127 expression inversely correlates with FoxP3 and suppressive function of human CD4+ T reg cells, J. Exp. Med. 203 (2006) 1701-1711.

[14] H.S. Kuehn, W. Ouyang, B. Lo, E.K. Deenick, J.E. Niemela, D.T. Avery, J.-N. Schickel, D.Q. Tran, J. Stoddard, Y. Zhang, D.M. Frucht, B. Dumitriu, P. Scheinberg, L.R. Folio, C.A. Frein, S. Price, C. Koh, T. Heller, C.M. Seroogy, A. Huttenlocher, V.K. Rao, H.C. Su, D. Kleiner, L.D. Notarangelo, Y. Rampertaap, K.N. Olivier, J. McElwee, J. Hughes, S. Pittaluga, J.B. Oliveira, E. Meffre, T.A. Fleisher, S.M. Holland, M.J. Lenardo, S.G. Tangye, G. Uzel, Immune dysregulation in human subjects with heterozygous germline mutations in CTLA4, Science (80). 345 (2014) 1623–1627.

[15] W.S. Thompson, M.L. Pekalski, H.Z. Simons, D.J. Smyth, X. Castro-Dopico, H. Guo, C. Guy, D.B. Dunger, S. Arif, M. Peakman, C. Wallace, L.S. Wicker, J.A. Todd, R.C. Ferreira, Multi-parametric flow cytometric and genetic investigation of the peripheral B cell compartment in human type 1 diabetes, Clin. Exp. Immunol. 177 (2014) 571–585.

[16] D.B. Rainbow, X. Yang, O. Burren, M.L. Pekalski, D.J. Smyth, M.D.R. Klarqvist, C.J. Penkett, K. Brugger, H. Martin, J.A. Todd, C. Wallace, L.S. Wicker, Epigenetic

589 analysis of regulatory T cells using multiplex bisulfite sequencing, Eur. J. Immunol. 45
590 (2015) 3200–3203.
591 [17] S.A. McClymont, A.L. Putnam, M.R. Lee, J.H. Esensten, W. Liu, M.A. Hulme, U.
592 Hoffmüller, U. Baron, S. Olek, J.A. Bluestone, T.M. Brusko, Plasticity of Human
593 Regulatory T Cells in Healthy Subjects and Patients with Type 1 Diabetes, J.
594 Immunol. 186 (2011) 3918–3926.
595 [18] A. Zóka, G. Barna, A. Somogyi, G. Műzes, Á. Oláh, Z. Al-Aissa, O. Hadarits, K. Kiss,
596 G. Firneisz, Extension of the CD4+Foxp3+CD25−/low regulatory T-cell
597 subpopulation in type 1 diabetes mellitus, Autoimmunity. 48 (2015) 289–297.
598 [19] D. Bending, A.M. Pesenacker, S. Ursu, Q. Wu, H. Lom, B. Thirugnanabalan, L.R.
599 Wedderburn, Hypomethylation at the Regulatory T Cell–Specific Demethylated
600 Region in CD25hi T Cells Is Decoupled from FOXP3 Expression at the Inflamed Site
601 in Childhood Arthritis, J. Immunol. 193 (2014) 2699–2708.
602 [20] M. Vukmanovic-Stejic, Y. Zhang, J.E. Cook, J.M. Fletcher, A. McQuaid, J.E. Masters,
603 M.H.A. Rustin, L.S. Taams, P.C.L. Beverley, D.C. Macallan, A.N. Akbar, Human
604 CD4+ CD25hi Foxp3+ regulatory T cells are derived by rapid turnover of memory
605 populations in vivo , J. Clin. Invest. 116 (2006) 2423–2433.
606 [21] J.B. Bollyky, S.A. Long, M. Fitch, P.L. Bollyky, M. Rieck, R. Rogers, P.L. Samuels,
607 S. Sanda, J.H. Buckner, M.K. Hellerstein, C.J. Greenbaum, Evaluation of in vivo T
608 cell kinetics: use of heavy isotope labelling in type 1 diabetes, Clin. Exp. Immunol.
609 172 (2013) 363–374.
610 [22] T. Asano, Y. Meguri, T. Yoshioka, Y. Kishi, M. Iwamoto, M. Nakamura, Y. Sando, H.
611 Yagita, J. Koreth, H.T. Kim, E.P. Alyea, P. Armand, C.S. Cutler, V.T. Ho, J.H. Antin,
612 R.J. Soiffer, Y. Maeda, M. Tanimoto, J. Ritz, K. Matsuoka, PD-1 modulates regulatory
613 T cell homeostasis during low-dose IL-2 therapy, Blood. 129 (2017) 2186-2197.
614 [23] A.H. Sharpe, E.J. Wherry, R. Ahmed, G.J. Freeman, The function of programmed cell
615 death 1 and its ligands in regulating autoimmunity and infection, Nat Immunol. 8
616 (2007) 239–245.
617 [24] B.T. Fife, J.A. Bluestone, Control of peripheral T-cell tolerance and autoimmunity via
618 the CTLA-4 and PD-1 pathways, Immunol. Rev. 224 (2008) 166–182.
619 [25] L.M. Francisco, P.T. Sage, A.H. Sharpe, The PD-1 pathway in tolerance and
620 autoimmunity, Immunol. Rev. 236 (2010) 219–242.

621 [26] D. Franceschini, M. Paroli, V. Francavilla, M. Videtta, S. Morrone, G. Labbadia, A.
622 Cerino, M.U. Mondelli, V. Barnaba, PD-L1 negatively regulates CD4+CD25+Foxp3+
623 Tregs by limiting STAT-5 phosphorylation in patients chronically infected with HCV ,
624 J. Clin. Invest. 119 (2009) 551–564.
625 [27] P.T. Sage, L.M. Francisco, C. V Carman, A.H. Sharpe, The receptor PD-1 controls
626 follicular regulatory T cells in the lymph nodes and blood, Nat Immunol. 14 (2013)
627 152–161.
628 [28] M. Wong, A. La Cava, B.H. Hahn, Blockade of Programmed Death-1 in Young (New
629 Zealand Black × New Zealand White)F1 Mice Promotes the Suppressive Capacity of
630 CD4+ Regulatory T Cells Protecting from Lupus-like Disease, J. Immunol. 190 (2013)
631 5402–5410.
632

Figure legends

Fig. 1. Frequency of CD25^{low}FOXP3^{+} cells is increased in patients with autoimmune disease. (**A**) Patterns of CD25 and FOXP3 expression among CD127^{low} CD4^{+} T cells from healthy donors and patients with autoimmune manifestations. **(B)** Gating strategy for the delineation of the T-cell subsets characterised in this study. Distribution of FOXP3^{+} cells among: (i) CD127^{low}CD25^{high} conventional Tregs (depicted in blue); and (ii) CD127^{low}CD25^{low} T cells (depicted in red). The vertical dotted line represents the threshold for the gating of FOXP3^{+} cells (histograms). **(C, D)** Scatter plots depict the frequency (geometric mean +/- 95% CI) of FOXP3^{+} cells among CD127^{low}CD25^{low} T cells in SLE patients (N = 32 patients vs 24 healthy donors) and combined immunodeficiency patients with active autoimmunity (N = 7 patients vs 6 healthy donors) (**C**); or in a cohort of T1D patients (N = 62; depicted by red circles) and healthy donors (N = 54; depicted by black squares) (**D**). *P* values were calculated using two-tailed unpaired t-tests. The initial CD4^{+} T cell gate (CD4 versus dead cell exclusion dye) was derived from a lymphocyte gate (defined on forward and side scatter) followed by single-cell discrimination**.** HC, healthy controls; T1D, type 1 diabetes patients; SLE, systemic lupus erythematosus patients; CID, combined immunodeficiency patients.

Fig. 2. CD25^{low}FOXP3^{+} cells are demethylated at the *FOXP3* Treg-specific demethylated region (TSDR). (A) Gating strategy for FACS sorting of four CD4^{+} T-cell subsets: (i) CD127^{low}CD25^{low}FOXP3^{-} (depicted in green), (ii) CD127^{low}CD25^{low}FOXP3^{+} (depicted in red), (iii) CD127^{low}CD25^{high}FOXP3^{-} (depicted in grey), and (iv) CD127^{low}CD25^{high}FOXP3^{+} (depicted in blue). **(B)** Frequency (mean +/− SEM) of reads demethylated at eight or nine of the nine interrogated CpG sites in the *FOXP3* TSDR. The data were obtained from sorted cells from four independent healthy donors. **(C)** Graphic depicts the proportion of demethylated reads at the nine interrogated CpG sites from the *FOXP3* TSDR in one illustrative donor. Each horizontal line represents one sequencing read, with light green representing a methylated read (C) and dark green representing a demethylated read (T). Note that the plot is representative of a male donor. For female donors, X-chromosome inactivation causes half of the reads to be methylated and a correction factor of two was applied to obtain the frequency of demethylated reads.

Fig. 3. CD25^{low}FOXP3^{+} T cells display an antigen-experienced phenotype. (A, B) Representative histograms and summary scatter plots depict the frequency (geometric mean +/- 95% CI) of CD45RA^{-} memory T cells amongst the CD25^{low}FOXP3^{-} and CD25^{low}FOXP3^{+} subsets in a population of 24 adult (median age = 42 years) healthy donors (**A**) or in a population of 116 younger (median age = 14 years) T1D patients (N = 62) and healthy donors (N = 54) (**B**). **(C, D)** Representative histograms and the frequency distribution (geometric mean +/- 95% CI) of Ki-67^{+} (**C**) and PD-1^{+} (**D**) cells in the CD45RA^{-} compartment of the four assessed immune subsets. *P* values were calculated using two-tailed paired t-tests comparing the frequency of the assessed immune subsets from the same individual. Gating strategy to delineate: (i) CD127^{low}CD25^{low}FOXP3^{-} (highlighted in green), (ii) CD127^{low}CD25^{low}FOXP3^{+} (highlighted in red), (iii) CD127^{low}CD25^{high}FOXP3^{-} (highlighted in grey), and (iv) CD127^{low}CD25^{high}FOXP3^{+} (highlighted in blue) CD4^{+} T cells is depicted in Figure 2A.

Fig. 4. CD25^{low}FOXP3^{+} cells show reduced expression of several conventional Treg markers. (A) Representative histograms depict the distribution of the expression of the conventional Treg markers HELIOS, TIGIT, CD15s and CTLA-4 amongst: (i) CD127^{low}CD25^{low}FOXP3^{-} (highlighted in green), (ii) CD127^{low}CD25^{low}FOXP3^{+} (highlighted in red), (iii) CD127^{low}CD25^{high}FOXP3^{-} (highlighted in grey), and (iv) CD127^{low}CD25^{high}FOXP3^{+} (highlighted in blue) memory CD4^{+} T cells. **(B)** Scatter plots depict the distribution (geometric mean +/- 95% CI) of HELIOS (n = 24), TIGIT (n = 24), CD15s (n = 24) and CTLA-4 (n = 13) in the CD45RA^{-} compartment of the four assessed immune subsets. **(C)** Expression of FOXP3 (geometric mean +/- 95% CI) was measured in the CD25^{low}FOXP3^{+} (depicted by red squares) and CD25^{high}FOXP3^{+} (depicted by blue circles) subsets from 24 healthy donors. *P* values were calculated using two-tailed paired t-tests comparing the assessed immunophenotypes between CD25^{low}FOXP3^{-} and the other three delineated subsets from the same individual. MFI, mean fluorescence intensity.

Fig. 5. HELIOS^{+}CD45RA^{-} CD25^{low}FOXP3^{+} cells are demethylated at TSDR as much as conventional HELIOS^{+}CD45RA^{-} CD25^{high}FOXP3^{+} Tregs. Frequency (mean +/- SEM) of reads demethylated at eight or nine of the nine interrogated CpG sites in the *FOXP3* TSDR in

CD45RA$^-$ CD25^{low}FOXP3$^+$ cells and CD45RA$^-$ CD25^{high}FOXP3$^+$ Tregs stratified by the expression of HELIOS. The data were obtained from sorted cells from three independent healthy donors.

Fig. 6. HELIOS$^+$CD45RA$^-$ CD25^{low}FOXP3$^+$ cells show impaired production of IL-2 and IFN-γ. (A) Gating strategy to delineate the CD45RA$^-$HELIOS$^+$ subset of: (i) CD127^{low}CD25^{low}FOXP3$^+$ (highlighted in red), (ii) CD127^{low}CD25^{high}FOXP3$^+$ (highlighted in blue), and (iii) CD127$^+$CD25$^{low/+}$FOXP3$^-$ HELIOS$^-$ conventional (Conv) effector (highlighted in black) subsets of CD4$^+$ T cells. **(B, C)** Bar graphs depict the frequency (mean +/- 95% CI) of IL-2$^+$ and IFN-γ$^+$ cells in the CD45RA$^-$HELIOS$^+$ compartment (or the CD45RA$^-$HELIOS$^-$ compartment in the case of the conventional effector T cells) of the five assessed immune subsets depicted in panel A. Cytokine production was assessed in one single batch of ten donors. *P* values were calculated using two-tailed paired t-tests. FACS gating plots depict data from one illustrative donor. ** $P < 0.01$, *** $P < 0.001$.

Fig. Proliferating Ki-67$^+$ CD127^{low}CD25^{high} Tregs correlate with the frequencies of the CD127^{low}CD25^{low} and CD127^{low}CD25^{high} HELIOS$^+$FOXP3$^+$subsets. (A, B) Data shown depict the correlation between the frequency within CD45RA$^-$ CD4$^+$ T cells of in-cycle (Ki-67$^+$) CD4$^+$CD45RA$^-$ CD127^{low}CD25^{high} Tregs (FOXP3$^+$HELIOS$^+$) and the frequency of either CD25^{low} FOXP3$^+$HELIOS$^+$ T cells (A) or conventional CD25^{high} FOXP3$^+$HELIOS$^+$ Tregs (B). (C) Data shown depict the correlation between the frequencies of circulating CD4$^+$CD45RA$^-$ CD25^{low} FOXP3$^+$HELIOS$^+$ and CD25^{high} FOXP3$^+$HELIOS$^+$ T cells. Frequencies of the assessed immune subsets were measured in PBMCs from healthy volunteers from two independent cohorts: cohort 1 containing 24 donors (depicted in red) and cohort 2 containing 112 donors (depicted in black). The r^2 values represent the coefficient of determination of the linear regression in the combined cohorts, and the *P* values correspond to the F statistic testing the null hypothesis that the slope of the linear regression analysis is equal to 0.

Supplement

Supplementary Table 1. Antibodies and immunostaining panels used for flow cytometry. Detailed description of the fluorochrome-conjugated antibodies and immunostaining panels used in this study.

Supplementary Fig. 1. Frequency of $CD127^{low}CD25^{low}$ $FOXP3^{+}$ T cells is increased in T1D patients. (**A**) Scatter plot depicts the total frequency (geometric mean +/- 95% CI) of $CD25^{low}FOXP3^{+}$ cells out of $CD4^{+}$ T cells in our discovery cohort of 62 T1D patients (depicted by red circles) and 54 healthy controls (depicted by black squares) (**B**) Scatter plots depict the frequency (geometric mean +/- 95% CI) of $FOXP3^{+}$ cells from $CD127^{low}CD25^{low}$ T cells in: (i) an independent replication cohort consisting of 15 T1D patients and 15 healthy controls. *P* values were calculated using two-tailed unpaired t-tests comparing the geometric mean of the assessed immune subsets between T1D patients and healthy controls (HC).

Supplementary Fig. 2. Minimal increase in the frequency of $CD127^{low}CD25^{high}$ $FOXP3^{+}$ T cells in T1D patients. Scatter plot depicts the total frequency (geometric mean +/- 95% CI) of $CD25^{high}FOXP3^{+}$ cells (classical Tregs) out of $CD4^{+}$ T cells in our discovery cohort of 62 T1D patients (depicted by red circles) and 54 healthy controls (depicted by black squares). *P* values were calculated using two-tailed unpaired t-tests comparing the geometric mean of $CD25^{high}FOXP3^{+}$ Tregs between T1D patients and healthy controls (HC).

Supplementary Fig. 3. HELIOS expression defines distinct $FOXP3^{+}$ subsets. Scatter plots depict the distribution (geometric mean +/- 95% CI) of TIGIT (n = 24), CD15s (n = 24), CD45RA (n = 24), CTLA-4 (both frequency and MFI of the positive fraction; n = 13) and FOXP3 MFI (n = 24) in the $HELIOS^{+}$ and $HELIOS^{-}$ fractions of the (i) $CD25^{low}FOXP3^{+}$ T cells (depicted in red) and (ii) conventional $CD25^{low}FOXP3^{+}$ Tregs (depicted in blue). *P* values were calculated using two-tailed paired t-tests.

Supplementary Fig. 4. The frequency of $HELIOS^{+}$ $CD25^{low}FOXP3^{+}$ cells is increased in patients with autoimmune disease. (**A, B**) Scatter plots depict the distribution (geometric mean +/- 95% CI) of $HELIOS^{+}FOXP3^{+}$ cells among $CD127^{low}CD25^{low}$ T cells in SLE

patients (N = 32 patients vs 24 healthy donors) and combined immunodeficiency (CID) patients with active autoimmunity (N = 7 patients vs 6 healthy donors) (**A**); and in a cohort of T1D patients (N = 62; depicted by red circles) and healthy donors (N = 54; depicted by black squares) (**B**). (**C, D**) Scatter plots depict the distribution (geometric mean +/- 95% CI) of HELIOS^{+} cells within CD25^{low}FOXP3^{+} T cells in the cohort of SLE and CID patients (**C**) and in the cohort of T1D patients (**D**). *P* values were calculated using two-tailed unpaired t-tests comparing the geometric mean of the assessed immune subsets between patients and the respective healthy control groups. .HC, healthy controls; T1D, type 1 diabetes patients; SLE, systemic lupus erythematosus patients; CID, combined immunodeficiency patients; ns = non-significant.

Supplementary Fig. 5. Production of IFN-γ from HELIOS^{-}CD45RA^{-} CD127^{low}CD25^{low}FOXP3^{+} T cells is not altered in T1D patients. (A) Gating strategy illustrating the production of IFN-γ in the HELIOS^{-} and HELIOS^{+} CD45RA^{-} fractions of CD127^{low}CD25^{low}FOXP3^{+} cells. FACS gating plot is a representative example. **(B)** Plot depicts the distribution of the frequency (geometric mean +/- 95% CI) of IFN-γ^{+} HELIOS^{-} T cells in the CD45RA^{-} CD127^{low}CD25^{low}FOXP3^{+} population. Frequency of IFN-γ^{+} cells was compared between T1D patients (N = 62; depicted by red circles) and healthy donors (N = 54; depicted by black squares) following *in vitro* stimulation with phorbol-12-myristate-13-acetate (PMA) and ionomycin. (**C**) Plot depicts the distribution of the frequency (geometric mean +/- 95% CI) of IFN-γ^{+} HELIOS^{-} T cells in the CD45RA^{-} CD127^{low}CD25^{low}FOXP3^{+} population out of total CD4 T cells from the same donors as in (**B**). *P* values were calculated by linear regression of the log-transformed data, including batch as a covariate. HC, healthy controls; T1D, type 1 diabetic patients.

Figure 1

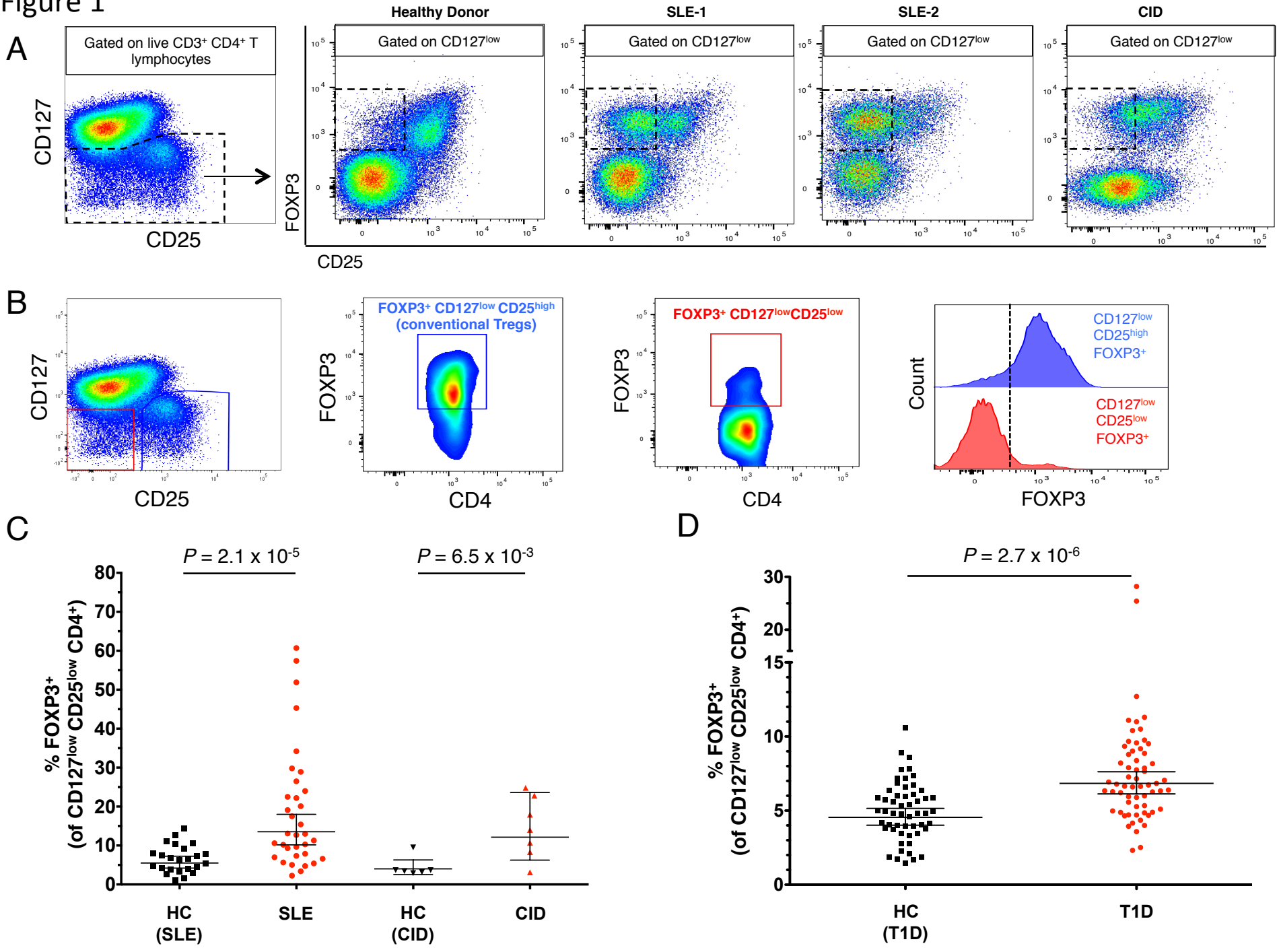
A
Gated on live CD3+ CD4+ T lymphocytes
CD127
CD25
Healthy Donor
SLE-1
SLE-2
CID
Gated on CD127low
FOXP3
CD25
B
CD127
CD25
FOXP3+ CD127low CD25high (conventional Tregs)
FOXP3
CD4
FOXP3+ CD127lowCD25low
FOXP3
CD4
Count
CD127low CD25high FOXP3+
CD127low CD25low FOXP3+
FOXP3
C
P = 2.1 x 10-5
P = 6.5 x 10-3
% FOXP3+ (of CD127low CD25low CD4+)
HC (SLE)
SLE
HC (CID)
CID
D
P = 2.7 x 10-6
% FOXP3+ (of CD127low CD25low CD4+)
HC (T1D)
T1D

Figure 2

A

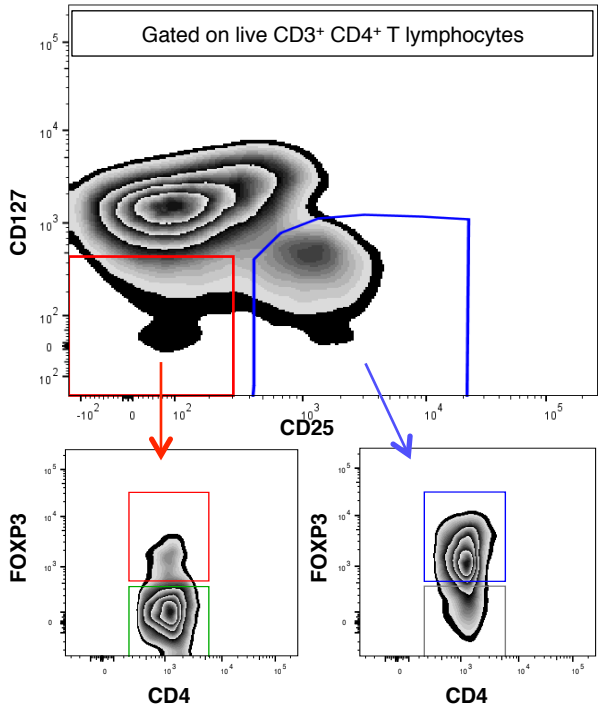
Gated on live CD3+ CD4+ T lymphocytes
CD127
CD25
FOXP3
CD4
FOXP3
CD4

B

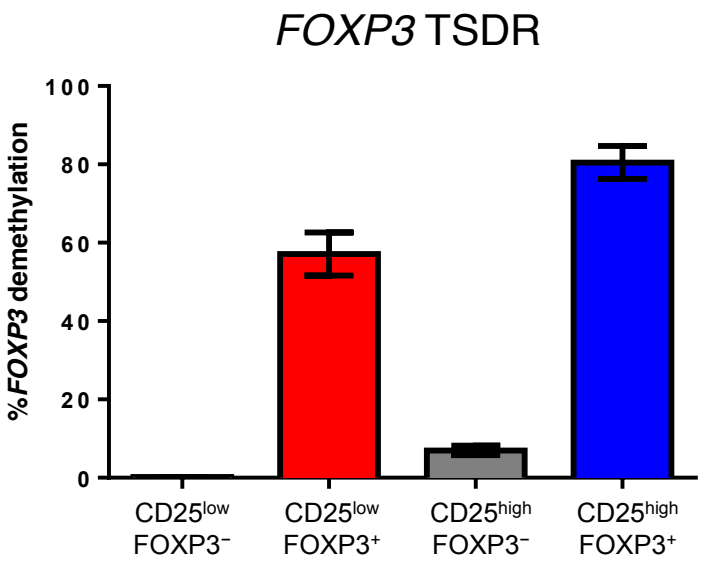
FOXP3 TSDR
%FOXP3 demethylation
100
80
60
40
20
0
CD25low FOXP3−
CD25low FOXP3+
CD25high FOXP3−
CD25high FOXP3+

C

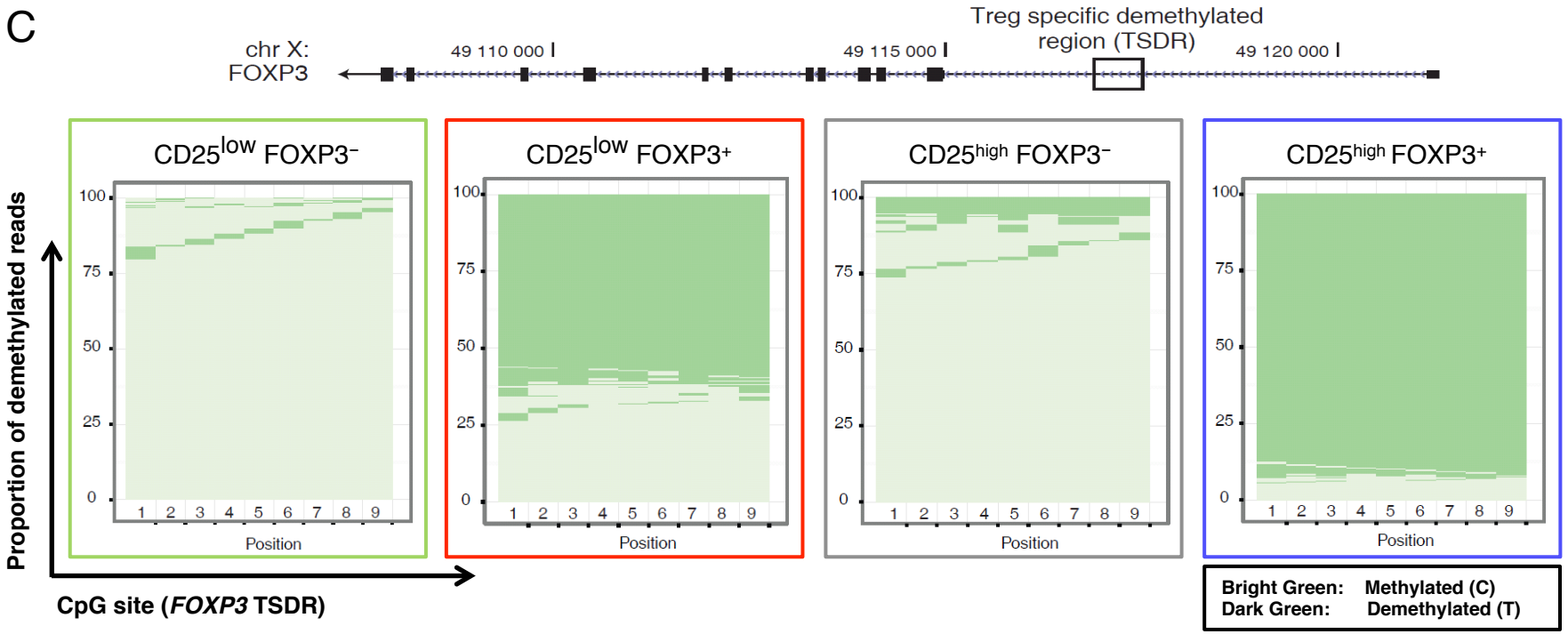
chr X:
FOXP3
49 110 000
49 115 000
Treg specific demethylated region (TSDR)
49 120 000
CD25low FOXP3−
CD25low FOXP3+
CD25high FOXP3−
CD25high FOXP3+
Proportion of demethylated reads
100
75
50
25
0
1 2 3 4 5 6 7 8 9
Position
CpG site (FOXP3 TSDR)
Bright Green: Methylated (C)
Dark Green: Demethylated (T)

Figure 3

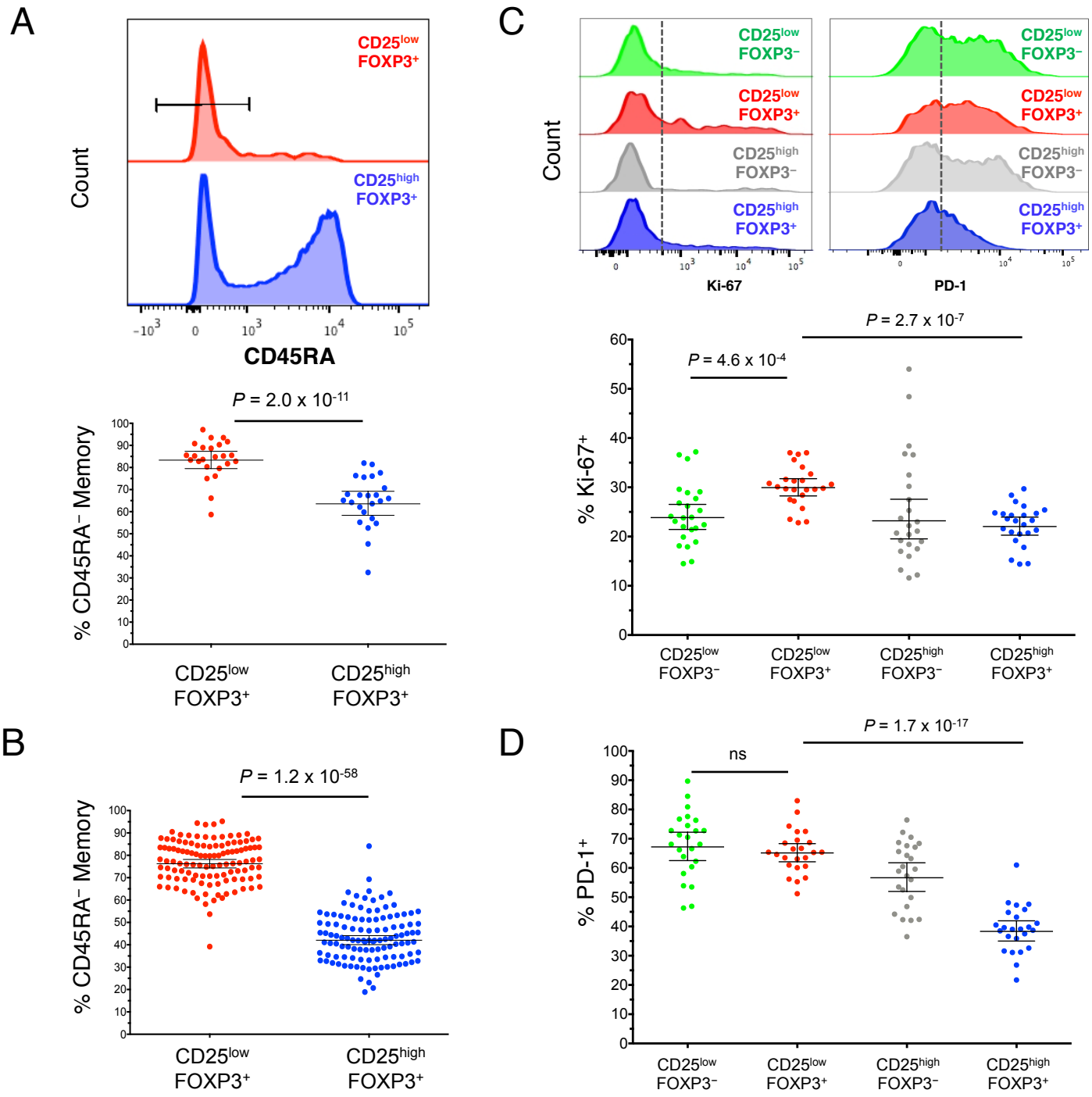
A
CD25low FOXP3+
CD25high FOXP3+
Count
CD45RA
P = 2.0 x 10-11
% CD45RA- Memory
CD25low FOXP3+
CD25high FOXP3+
B
P = 1.2 x 10-58
% CD45RA- Memory
CD25low FOXP3+
CD25high FOXP3+
C
CD25low FOXP3-
CD25low FOXP3+
CD25high FOXP3-
CD25high FOXP3+
Count
Ki-67
PD-1
P = 4.6 x 10-4
P = 2.7 x 10-7
% Ki-67+
CD25low FOXP3-
CD25low FOXP3+
CD25high FOXP3-
CD25high FOXP3+
D
ns
P = 1.7 x 10-17
% PD-1+
CD25low FOXP3-
CD25low FOXP3+
CD25high FOXP3-
CD25high FOXP3+

Figure 4

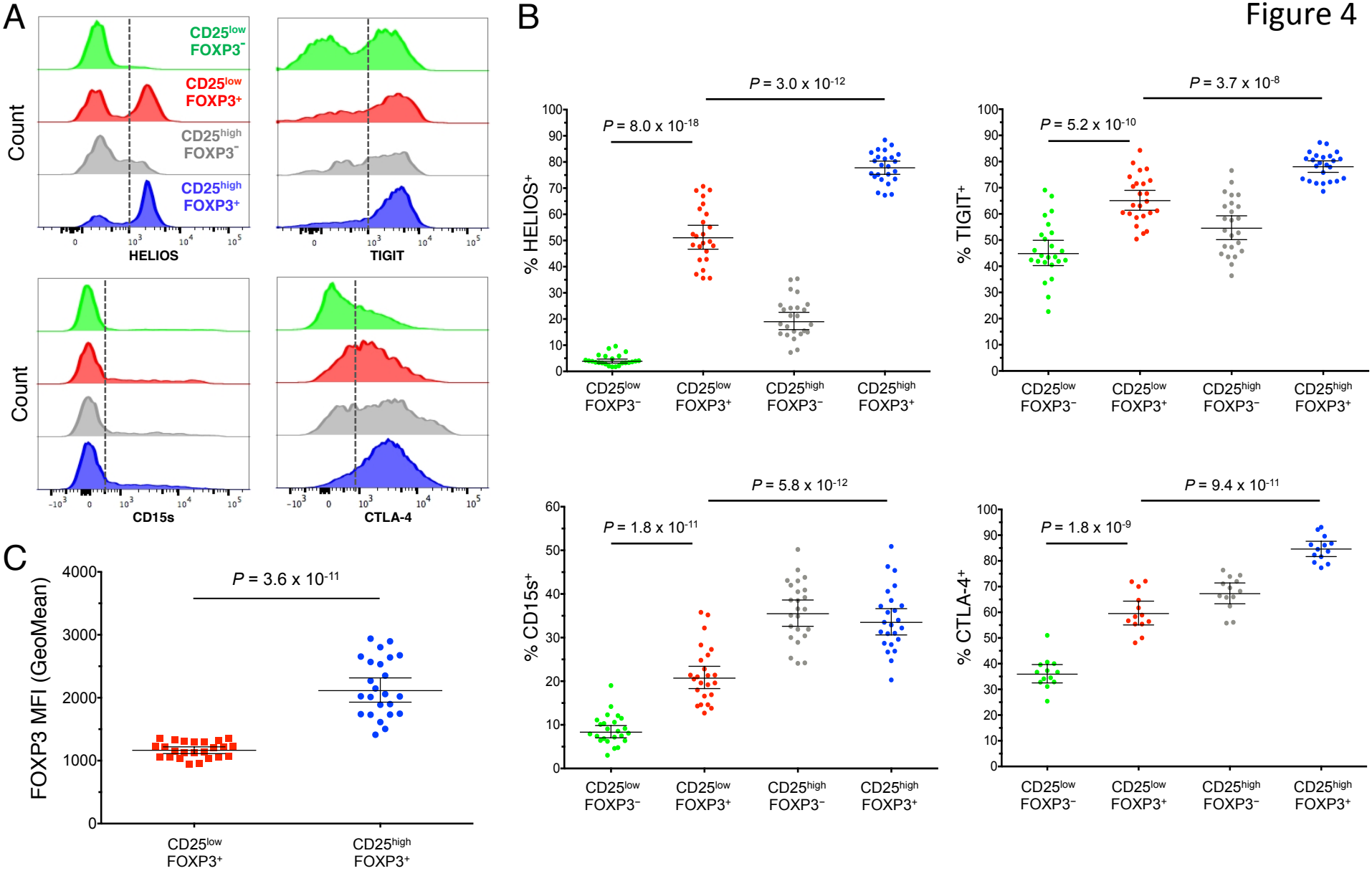
A
Count
CD25low FOXP3-
CD25low FOXP3+
CD25high FOXP3-
CD25high FOXP3+
HELIOS
TIGIT
CD15s
CTLA-4
B
% HELIOS+
P = 3.0 x 10-12
P = 8.0 x 10-18
% TIGIT+
P = 3.7 x 10-8
P = 5.2 x 10-10
% CD15s+
P = 5.8 x 10-12
P = 1.8 x 10-11
% CTLA-4+
P = 9.4 x 10-11
P = 1.8 x 10-9
CD25low FOXP3−
CD25low FOXP3+
CD25high FOXP3−
CD25high FOXP3+
C
FOXP3 MFI (GeoMean)
P = 3.6 x 10-11

Figure 5

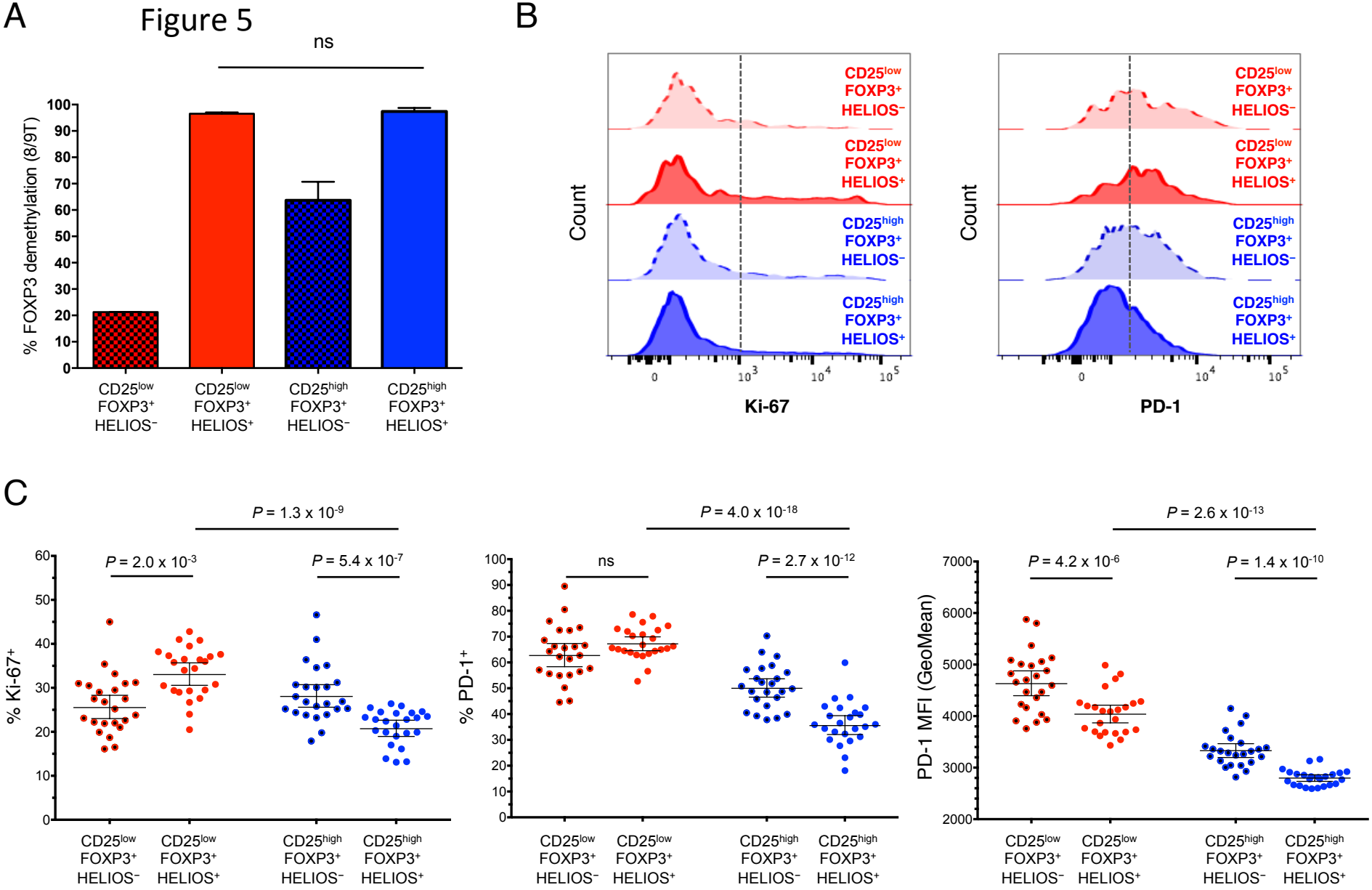
A
ns
% FOXP3 demethylation (8/9T)
100
90
80
70
60
50
40
30
20
10
0
CD25low FOXP3+ HELIOS−
CD25low FOXP3+ HELIOS+
CD25high FOXP3+ HELIOS−
CD25high FOXP3+ HELIOS+
B
Count
CD25low FOXP3+ HELIOS−
CD25low FOXP3+ HELIOS+
CD25high FOXP3+ HELIOS−
CD25high FOXP3+ HELIOS+
0
10^3
10^4
10^5
Ki-67
Count
CD25low FOXP3+ HELIOS−
CD25low FOXP3+ HELIOS+
CD25high FOXP3+ HELIOS−
CD25high FOXP3+ HELIOS+
0
10^4
10^5
PD-1
C
P = 1.3 x 10-9
P = 2.0 x 10-3
P = 5.4 x 10-7
% Ki-67+
60
50
40
30
20
10
0
CD25low FOXP3+ HELIOS−
CD25low FOXP3+ HELIOS+
CD25high FOXP3+ HELIOS−
CD25high FOXP3+ HELIOS+
P = 4.0 x 10-18
ns
P = 2.7 x 10-12
% PD-1+
100
90
80
70
60
50
40
30
20
10
0
CD25low FOXP3+ HELIOS−
CD25low FOXP3+ HELIOS+
CD25high FOXP3+ HELIOS−
CD25high FOXP3+ HELIOS+
P = 2.6 x 10-13
P = 4.2 x 10-6
P = 1.4 x 10-10
PD-1 MFI (GeoMean)
7000
6000
5000
4000
3000
2000
CD25low FOXP3+ HELIOS−
CD25low FOXP3+ HELIOS+
CD25high FOXP3+ HELIOS−
CD25high FOXP3+ HELIOS+

Figure 6

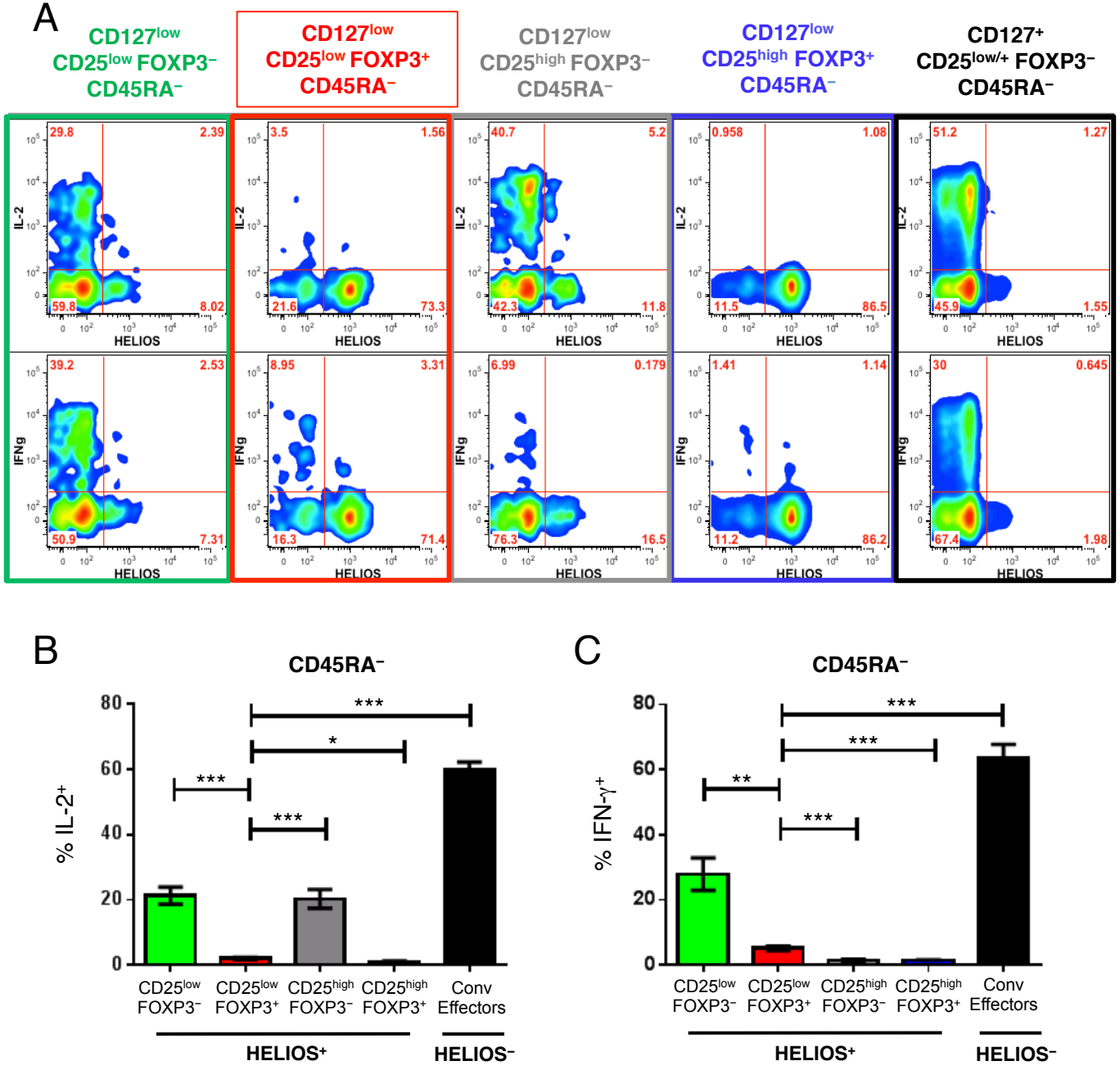
A
CD127low CD25low FOXP3− CD45RA−
CD127low CD25low FOXP3+ CD45RA−
CD127low CD25high FOXP3− CD45RA−
CD127low CD25high FOXP3+ CD45RA−
CD127+ CD25low/+ FOXP3− CD45RA−
IL-2
IFNg
HELIOS
29.8
2.39
59.8
8.02
3.5
1.56
21.6
73.3
40.7
5.2
42.3
11.8
0.958
1.08
11.5
86.5
51.2
1.27
45.9
1.55
39.2
2.53
50.9
7.31
8.95
3.31
16.3
71.4
6.99
0.179
76.3
16.5
1.41
1.14
11.2
86.2
30
0.645
67.4
1.98
B
CD45RA−
% IL-2+
CD25low FOXP3−
CD25low FOXP3+
CD25high FOXP3−
CD25high FOXP3+
Conv Effectors
HELIOS+
HELIOS−
C
CD45RA−
% IFN-γ+
CD25low FOXP3−
CD25low FOXP3+
CD25high FOXP3−
CD25high FOXP3+
Conv Effectors
HELIOS+
HELIOS−

Figure 7

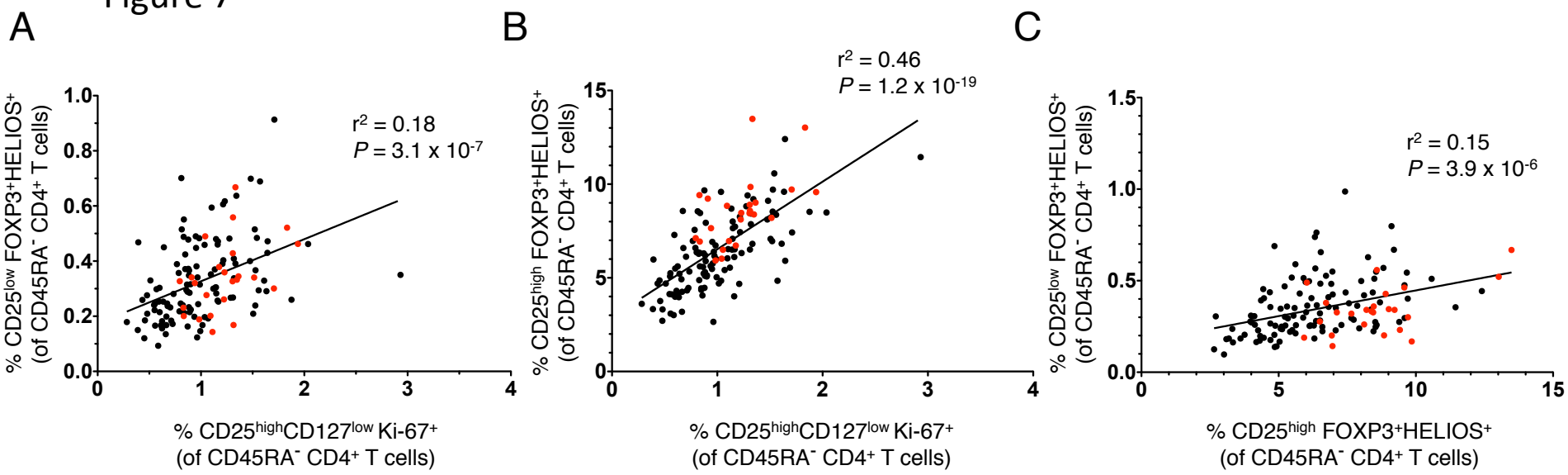
A
B
C
r² = 0.18
P = 3.1 x 10⁻⁷
r² = 0.46
P = 1.2 x 10⁻¹⁹
r² = 0.15
P = 3.9 x 10⁻⁶
% CD25low FOXP3+HELIOS+ (of CD45RA- CD4+ T cells)
% CD25high FOXP3+HELIOS+ (of CD45RA- CD4+ T cells)
% CD25high CD127low Ki-67+ (of CD45RA- CD4+ T cells)
% CD25high FOXP3+HELIOS+ (of CD45RA- CD4+ T cells)

Fig S1

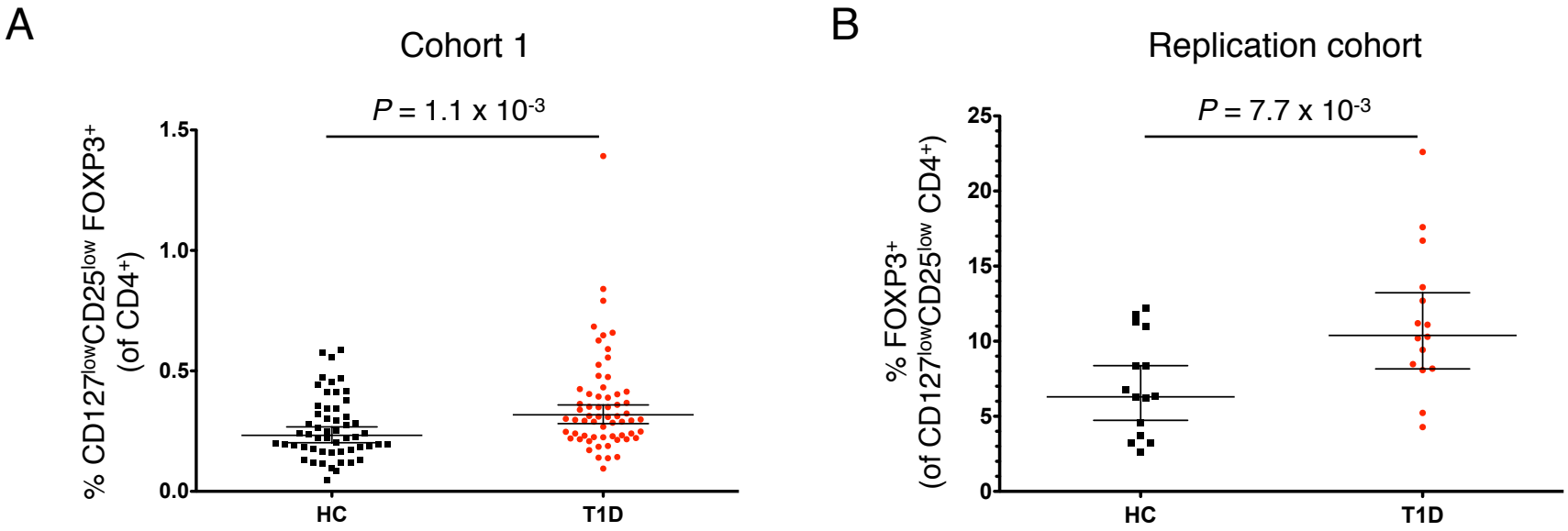
A
Cohort 1
P = 1.1 x 10-3
% CD127lowCD25low FOXP3+ (of CD4+)
1.5
1.0
0.5
0.0
HC
T1D
B
Replication cohort
P = 7.7 x 10-3
% FOXP3+ (of CD127lowCD25low CD4+)
25
20
15
10
5
0
HC
T1D

Fig S2

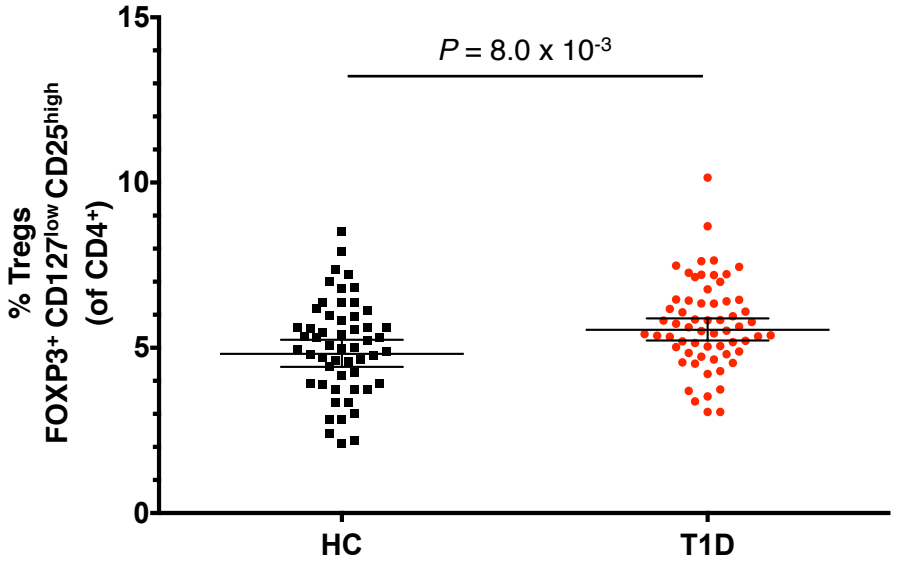

Fig S3

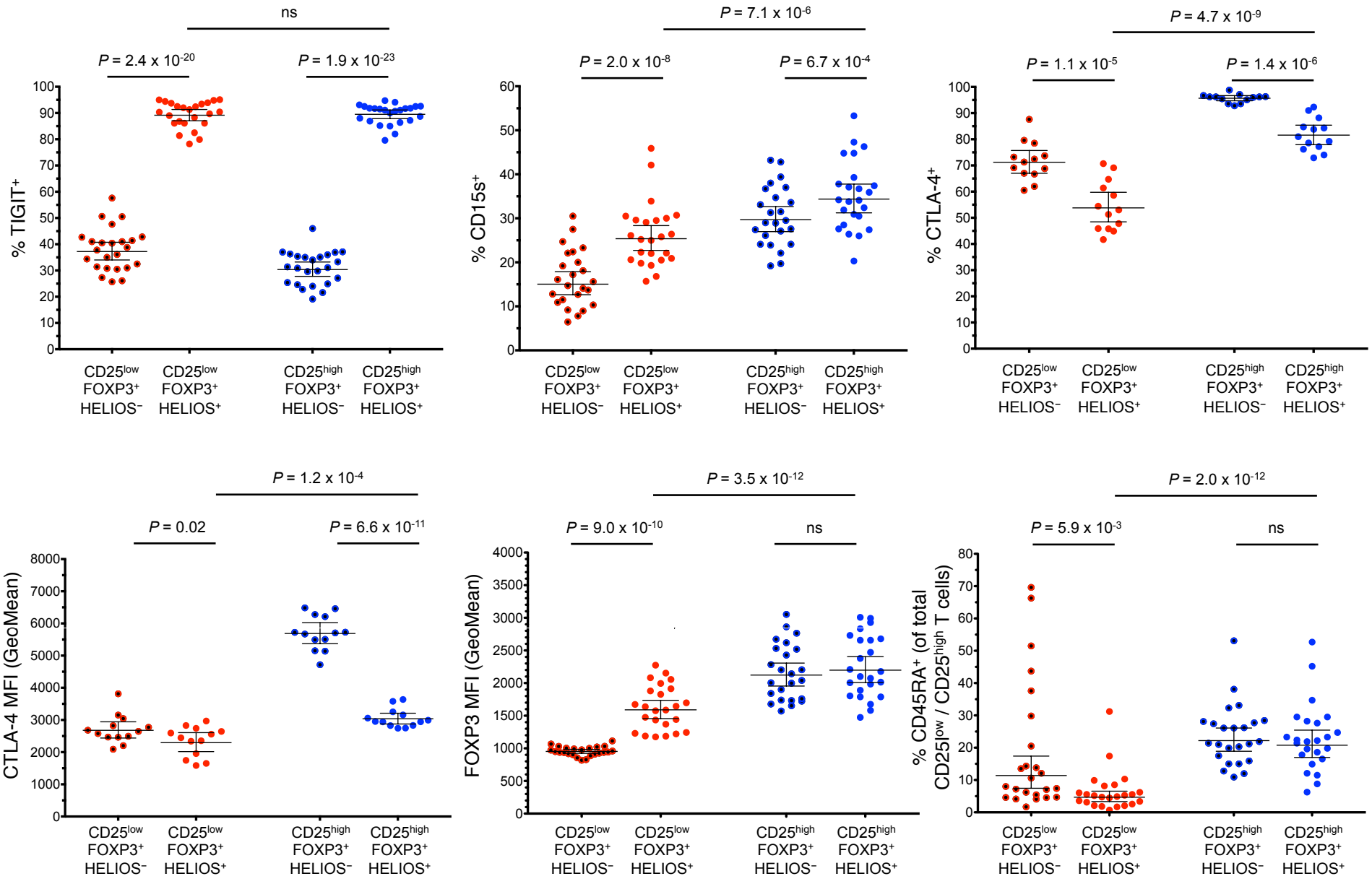
ns
P = 2.4 x 10-20
P = 1.9 x 10-23
% TIGIT+
P = 7.1 x 10-6
P = 2.0 x 10-8
P = 6.7 x 10-4
% CD15s+
P = 4.7 x 10-9
P = 1.1 x 10-5
P = 1.4 x 10-6
% CTLA-4+
P = 1.2 x 10-4
P = 0.02
P = 6.6 x 10-11
CTLA-4 MFI (GeoMean)
P = 3.5 x 10-12
P = 9.0 x 10-10
ns
FOXP3 MFI (GeoMean)
P = 2.0 x 10-12
P = 5.9 x 10-3
ns
% CD45RA+ (of total CD25low / CD25high T cells)
CD25low FOXP3+ HELIOS−
CD25low FOXP3+ HELIOS+
CD25high FOXP3+ HELIOS−
CD25high FOXP3+ HELIOS+

Fig S4

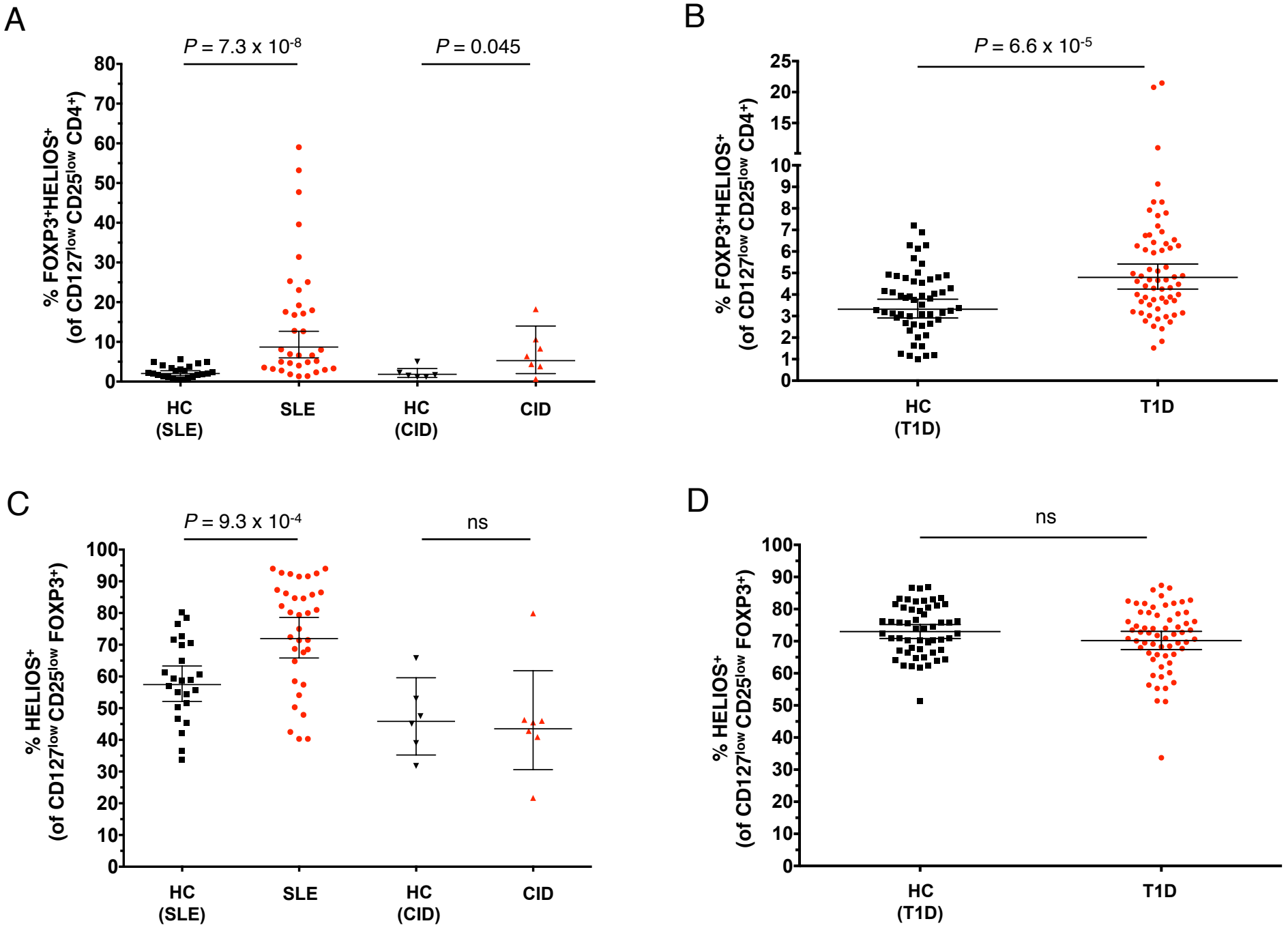
A
P = 7.3 x 10-8
P = 0.045
% FOXP3+HELIOS+ (of CD127low CD25low CD4+)
HC (SLE)
SLE
HC (CID)
CID
B
P = 6.6 x 10-5
% FOXP3+HELIOS+ (of CD127low CD25low CD4+)
HC (T1D)
T1D
C
P = 9.3 x 10-4
ns
% HELIOS+ (of CD127low CD25low FOXP3+)
HC (SLE)
SLE
HC (CID)
CID
D
ns
% HELIOS+ (of CD127low CD25low FOXP3+)
HC (T1D)
T1D

Fig S5

A

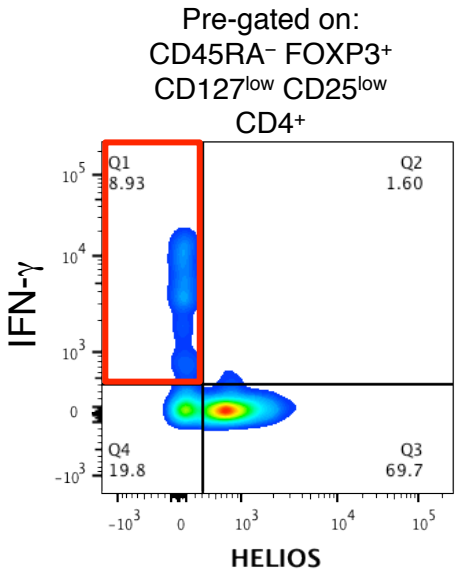
Pre-gated on:
CD45RA⁻ FOXP3⁺
CD127low CD25low
CD4⁺
Q1
8.93
Q2
1.60
Q4
19.8
Q3
69.7
IFN-γ
HELIOS

B

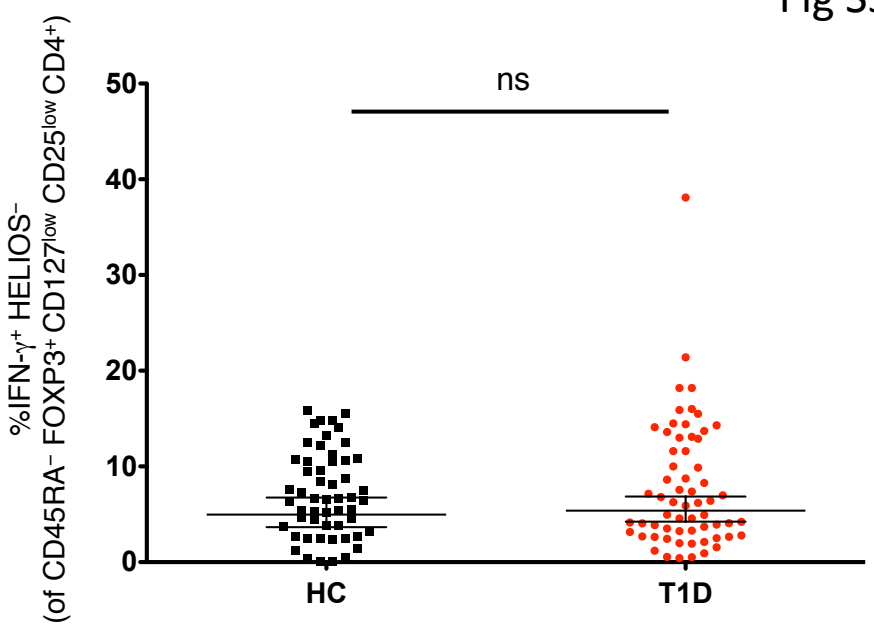
ns
%IFN-γ⁺ HELIOS⁻
(of CD45RA⁻ FOXP3⁺ CD127low CD25low CD4⁺)
50
40
30
20
10
0
HC
T1D

C

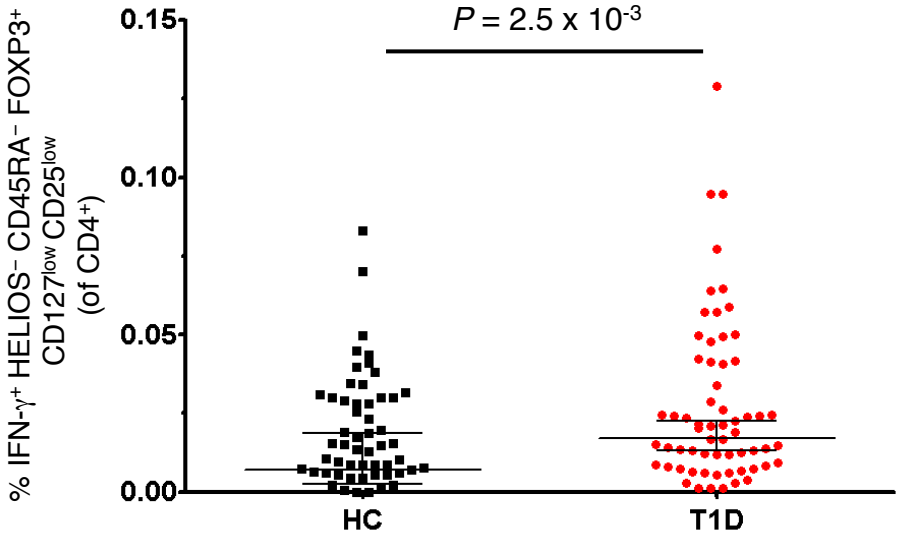
P = 2.5 x 10-3
% IFN-γ⁺ HELIOS⁻ CD45RA⁻ FOXP3⁺
CD127low CD25low
(of CD4⁺)
0.15
0.10
0.05
0.00
HC
T1D

Table 1. Baseline characteristics of study participants included in the association analyses

Cohort	N	Age (years)		Male N (%)	Duration of disease (months)	
		Median	Range		Median	Range
Autoimmune disease cohorts						
SLE	34	36	20-72	2 (5.9%)	N/A	N/A
Healthy controls (CBR) - cohort 1	24	42	22-62	1 (4.2%)	N/A	N/A
Healthy controls (CBR) - cohort 2	112	49	26-78	30 (26.8%)	N/A	N/A
CID	7	23	13-45	5 (71.4%)	N/A	N/A
Healthy controls (CBR)	6	34	17-47	4 (66.7%)	N/A	N/A
T1D discovery cohort						
T1D (D-GAP)[1]	49	13	6-34	32 (65.3%)	11	2-42
T1D (CBR)[2]	15	32	22-32	5 (33.3%)	198	6-276
T1D (combined)	*64*	*14*	*6-42*	*37 (58.0%)*	*22*	*2-276*
Unaffected Siblings (D-GAP)[3]	40	13	6-31	21 (52.5%)	N/A	N/A
Healthy Controls (CBR)	15	27	18-37	4 (26.7%)	N/A	N/A
Healthy controls (combined)	*55*	*15*	*6-37*	*28 (45.9%)*	*N/A*	*N/A*
T1D replication cohort						
T1D (CBR)	15	37	17-52	5 (33.3%)	N/A	N/A

Healthy Controls (CBR)	15	37	22-47	4 (26.7%)	240	24-240

Baseline characteristics for the study participants stratified by the study cohorts. [1]Newly diagnosed T1D patients (duration of disease <= 3 years) enrolled in the Diabetes - Genes, Autoimmunity and Prevention (D-GAP) study. [2]Long-standing adult T1D patients enrolled from the Cambridge BioResource (CBR). [3]First-degree sibling of a T1D patient, reporting no autoimmune disease and determined to be negative for the following T1D-associated autoantibodies: IAA, IA2, GAD and ZnT8. CID, Combined immunodeficiency; T1D, type 1 diabetes; SLE; systemic lupus erythematosus.